Laboratori Nazionali di Frascati

LNF-73/19

M. Grilli, E. Iarocci, P. Spillantini, V. Valente, R. Visentin, B. Borgia, F. Ceradini, M. Conversi, L. Paoluzi, R. Santonico, M. Nigro, L. Trasatti and G. T. Zorn:

MULTIHADRON PRODUCTION IN e^+e^- COLLISIONS AT HIGH ENERGY.

Nuovo Cimento 13A, 593 (1973).

IL NUOVO CIMENTO VOL. 13 A, N. 3 1 Febbraio 1973

Multihadron Production in e^+e^- Collisions at High Energy.

M. GRILLI, E. IAROCCI, P. SPILLANTINI, V. VALENTE and R. VISENTIN
Laboratori Nazionali di Frascati del CNEN - Frascati

B. BORGIA, F. CERADINI, M. CONVERSI, L. PAOLUZI and R. SANTONICO
Istituto di Fisica dell'Università - Roma
Istituto Nazionale di Fisica Nucleare - Sezione di Roma

M. NIGRO
Istituto di Fisica dell'Università - Padova
Istituto Nazionale di Fisica Nucleare - Sezione di Padova

L. TRASATTI and G. T. ZORN
Department of Physics and Astronomy, University of Maryland - Maryland, Md. (*)

(ricevuto il 9 Agosto 1972; manoscritto revisionato ricevuto il 28 Agosto 1972)

Summary. — Multihadron production by electron-positron colliding beams has been investigated for total centre-of-mass energies ranging from 1.2 to 2.4 GeV. The total cross-section, $\sigma_{tot} \equiv \sigma(e^+e^- \to \pi^+\pi^- + \text{anything})$, is of the order of $\sigma_{\mu\mu} \equiv \sigma(e^+e^- \to \mu^+\mu^-)$, with a threshold near 1 GeV. Partial cross-sections for the various channels are also derived. The cross-section of the specific channel $e^+e^- \to \pi^+\pi^-\pi^+\pi^-$ exhibits an energy dependence which is suggestive of a heavier vector meson, ρ' ($m_{\rho'} \approx 1.6$ GeV, $\Gamma_{\rho'} \approx 350$ MeV), having the same quantum numbers as the ρ-meson. An upper limit is given for the coupling constant $f_{\rho'}$ ($f_{\rho'}/4\pi < 18$, where $f_{\rho'} = m^2_{\rho'}e/g_{\gamma\rho'}$). Final states with G^+ parity are found to be much more abundant than those with G^- parity. The average multiplicity (charged plus neutral final-state pions) is found to be between 4 and 5 over all the energy range explored.

(*) Work partly supported by the U.S.A.E.C.

1. – Introduction.

The development of electron-positron storage rings of total energy in the GeV region has made possible the direct investigation of processes involving virtual photons in the deep timelike region. The reactions resulting from the e^+e^- collisions proceed in the one-photon approximation through a state of well-defined quantum numbers ($J^{PG} = 1^{--}$) and this selects the possible final states (1). Elegant and accurate experimental studies of well-established vector mesons with these quantum numbers (ρ, ω, φ) have become possible and have been carried out in recent years, at Novosibirsk with VEPP 2 (2) and at Orsay with ACO (3).

Investigations of this type at higher energy are of the greatest interest, not only because they represent a search for other possible resonances with higher masses, but also because of possible linkages with deep electron-proton inelastic scattering (4), as the asymptotic region is reached (*).

The successful operation of Adone (5), the Frascati 2×1.5 GeV e^+e^- storage ring, has made it possible to accomplish a first step along these lines. As will be seen later on in this article, this has been accomplished through the

---

(1) For a comprehensive discussion on the physics of high-energy e^+e^- colliding beams we refer the reader to a well-known paper by N. CABIBBO and R. GATTO: *Phys. Rev.*, **124**, 1577 (1961). For a survey of the experimental results obtained as of Sept. 1971 see M. CONVERSI: *Daresbury Study Week-End*, No. 4 (1971) p. 85. Results dealing specifically with hadron production in the GeV region have been recently reviewed in lectures delivered at the *International School of Yerevan Physical Institute*, see M. GRILLI: Frascati report LNF 71/100 (Dec. 1971). See also: C. BERNARDINI: *Proceedings of the International Symposium on Electron and Photon Interactions at High Energies* (Ithaca, 1971).

(2) V. E. BALAKIN, G. I. BUDKER, E. V. PAKHTUSOVA, V. A. SIDOROV, A. N. SKRINSKIJ, G. M. TUMAIKIN and A. G. KHABAKHPRASHEV: *Phys. Lett.*, **34** B, 328 (1971).

(3) See, also for previous reference: *a*) D. BENAKSAS, G. COSME, B. JEAN-MARIE, S. JULLIAN, F. LAPLANCE, J. LEFRANÇOIS, A. D. LIBERMAN, G. PARROUR, J. P. REPELLIN and G. SAUVAGE: *Phys. Lett.*, **39** B, 289 (1972); *b*) J. LEFRANÇOIS: *Proceedings of the International Symposium on Electron and Photon Interactions at High Energies* (Ithaca, N. Y., 1971), p. 51.

(4) See for instance: *a*) W. K. H. PANOFSKY: *Comments on Nuclear and Particle Physics*, **4**, No. 5 (1970); *b*) J. J. SAKURAI: invited paper at *Balaton Symposium on Hadron Spectroscopy* (Sept. 1970), in *Acta Phys. Hung.*, **31**, 5 (1972); *c*) S. D. DRELL: rapporteur talk at the *International Conference on Elementary Particles* (Amsterdam, 1971); *d*) J. D. BJORKEN: rapporteur talk at the *International Symposium on Electron and Photon Interactions at High Energy* (Ithaca, N. Y., 1971).

(*) This point will be discussed further in Sect. **11**.

(5) F. AMMAN, R. ANDREANI, M. BASSETTI, M. BERNARDINI, A. CATTONI, V. CHIMENTI, G. F. CORAZZA, D. FABIANI, E. FERLENGHI, A. MASSAROTTI, C. PELLEGRINI, M. PLACIDI, M. PUGLISI, F. SOSO, S. TAZZARI, F. TAZZIOLI and G. VIGNOLA: *Lett. Nuovo Cimento*, **1**, 729 (1969).

study of the multihadron reactions

$$e^+e^- \to m(h^+h^-) + n\,h^0, \tag{1}$$

where $m \geqslant 1$, $n \geqslant 0$, $m + n \geqslant 2$ and h^+, h^-, h^0 are assumed to be pions for reasons explained later. The investigation of the two-body hadronic process $e^+e^- \to h^+h^-$ has been performed by our group ($\mu\pi$) and the BCF group at Adone ([6]). The results on this reaction will be the subject of separate papers ([7]).

Multihadron production was observed at Adone, and independently at Novosibirsk, early in 1970. It was first reported at the Kiev International Conference ([8]). These preliminary results have been substantially confirmed by subsequent experimentation leading to better estimates ([6a,9-12]) of the cross-sections for the reactions (1).

([6]) *a*) B. BORGIA, M. CONVERSI, M. GRILLI, E. IAROCCI, M. NIGRO, L. PAOLUZI, P. SPILLANTINI, L. TRASATTI, V. VALENTE, R. VISENTIN and G. T. ZORN: Frascati LNF 71/62 (1971); presented at the *International Symposium on Electron and Photon Interactions at High Energies* (Ithaca, N. Y., 1971); *b*) V. ALLES-BORELLI, M. BERNARDINI, D. BOLLINI, T. MASSAM, L. MONARI, F. PALMONARI and A. ZICHICHI: invited talk (presented by A. ZICHICHI) in the *Proceedings of the International Conference of E.P.S. on Meson Resonances and Related Electromagnetic Phenomena* (Bologna, 1971).

([7]) *a*) V. ALLES-BORELLI, M. BERNARDINI, D. BOLLINI, P. L. BRUSINI, E. FIORENTINO, T. MASSAM, L. MONARI, F. PALMONARI, F. RIMONDI and A. ZICHICHI: CERN preprint, Geneva (May 1972); *b*) G. BARBIELLINI, F. CERADINI, M. CONVERSI, S. D'ANGELO, E. IAROCCI, G. GIANNOLI, M. GRILLI, M. NIGRO, L. PAOLUZI, R. SANTONICO, P. SPILLANTINI, L. TRASATTI, V. VALENTE, R. VISENTIN and G. T. ZORN: in progress.

([8]) *a*) G. BARBIELLINI, M. CONVERSI, M. GRILLI, A. MULACHIÉ, M. NIGRO, L. PAOLUZI P. SPILLANTINI, R. VISENTIN and G. T. ZORN: Frascati LNF-70/38 (1970); *Proceedings of the XV International Conference on High-Energy Physics* (Kiev, 1970), p. 704; *b*) B. BARTOLI, B. COLUZZI, F. FELICETTI, G. GOGGI, G. MARINI, F. MASSA, D. SCANNICCHIO, V. SILVESTRINI and F. VANOLI: *Nuovo Cimento*, **70** A, 615 (1970); *c*) V. E. BALAKIN, G. I. BUDKER, I. B. VASSERMAN, O. S. KOITMAN, L. M. KURDADZE, S. I. MISHNEV, A. P. OMUCHIN, S. I. SEREDNYAKOV, V. A. SIDOROV, A. N. SKRINSKY, G. M. TUMAIKIN, V. F. TURKIN, A. G. KHABAKHPASHEV and J. M. SHATUNOV: Novosibirsk Internal Report 62/70 (1970); *Proceedings of the XV International Conference on High-Energy Physics* (Kiev, 1970), p. 705; *d*) R. WILSON: *Proceedings of the XV International Conference on High-Energy Physics* (Kiev, 1970), p. 219.

([9]) *a*) « $\mu\pi$ group »: invited talk (presented by M. CONVERSI) in the *Proceedings of the International Conference of E.P.S. on Meson Resonances and Related Electromagnetic Phenomena* (Bologna, 1971); *b*) « $\gamma\gamma$ group »: invited talk (presented by G. SALVINI) in the *Proceedings of the International Conference of E.P.S. on Meson Resonances and Related Electromagnetic Phenomena* (Bologna, 1971).

([10]) B. BARTOLI, F. FELICETTI, G. MARINI, A. NIGRO, H. OGREN, N. SPINELLI, V. SILVESTRINI and F. VANOLI: *Phys. Lett.*, **36** B, 598 (1971).

([11]) B. BARTOLI, F. FELICETTI, G. MARINI, A. NIGRO, H. OGREN, V. SILVESTRINI and F. VANOLI: Frascati LNF-71/91 (1971) (submitted to *Phys. Rev.*).

([12]) C. BACCI, R. BALDINI-CELIO, G. CAPON, C. MENCUCCINI, G. P. MURTAS, G. PENSO, A. REALE, G. SALVINI, M. SPINETTI and B. STELLA: *Phys. Lett.*, **38** B, 551 (1972).

An interesting feature of the results obtained at Adone and reported in detail in the present article, is the relatively large value of the total cross-section for multihadron production. Over the centre-of-mass energy interval explored, $1.2 \leqslant 2E \leqslant 2.4$ GeV (where $2E = E_+ + E_-$ is the total energy of the colliding beams) this cross-section appears to be comparable with, or, at highest energies, possibly greater than the cross-section $\sigma_{\mu\mu}$ for e^+e^- annihilation into muon pairs. We recall that $\sigma_{\mu\mu} = 21/E^2$ nb (1 nb $= 10^{-33}$ cm^2) if E is expressed in GeV.

Unfortunately, due mostly to the rather large errors associated with the present data, it is difficult to discern possible structures in the energy dependence of σ_{tot}. Nevertheless, for the specific annihilation channel which has only four charged pions in the final state, our group has observed a broad peak ([13]) in the energy dependence of the production cross-section. The observed behaviour of the cross-section is consistent with the hypothesis of a ρ'-meson ([14]) of mass $m_{\rho'} = \sim 1.6$ GeV and width $\Gamma_{\rho'} = \sim 350$ MeV. Such a hypothesis will be further discussed later in this article, also in the light of other recent experimental results obtained at SLAC (*).

After a description of the experimental apparatus in Sect. **2**, the results of the measurements performed with electrons of known energies in order to obtain a calibration of the apparatus itself are given in Sect. **3**. The subsequent Sect. **4** describes the scanning and the event selection. Background problems are discussed in Sect. **5**, and Sect. **6** is devoted to a phenomenological classification of events. In Sect. **7** the nature of the secondary particles and the reactions are analysed and in Sect. **8** a Monte Carlo simulation of the experiment is described. In view of the possible existence of a ρ'-meson, a detailed analysis of the specific reaction $e^+e^- \to \pi^+\pi^-\pi^+\pi^-$ is made in Sect. **9**. The results are presented in Sect. **10** and discussed in Sect. **11**, which ends with a summary list of conclusions.

2. – Experimental apparatus.

The experiment was carried out at one of the four experimental straight sections of Adone. Measurements were made at values of the beam energy E in the range $(0.6 \div 1.2)$ GeV. The beams collided head-on in the centre of the experimental straight section. The collision region was assumed to have a Gaussian distribution in all directions. Its transverse dimensions were of the

---

([13]) G. BARBARINO, F. CERADINI, M. CONVERSI, M. GRILLI, E. IAROCCI, M. NIGRO, L. PAOLUZI, R. SANTONICO, P. SPILLANTINI, L. TRASATTI, V. VALENTE, R. VISENTIN and G. T. ZORN: *Lett. Nuovo Cimento*, **3**, 689 (1972).

([14]) A. BRAMON and M. GRECO: *Lett. Nuovo Cimento*, **3**, 693 (1972).

(*) We wish to thank Prof. J. J. SAKURAI for communicating to one of us (M.C.) the preliminary results of the SLAC experiment based on use of a back-scattered laser photon beams (see Sect. **11**).

order of 1 mm, while its longitudinal standard deviation was found by us ([15]) to be $\delta = (20 \pm 1.5)$ cm at $E = 1$ GeV, in agreement with the measurements made by the machine group ([16]). The quantity δ increased with energy ([17]) approximately as $E^{\frac{3}{2}}$. The collision time of the e^+ and e^- bunches was ~ 2 ns and the time between two consecutive collisions was ~ 117 ns. In the beam energy interval covered during this experiment, the machine luminosity L increased steeply with the beam energy (*). At $E = 1$ GeV/beam $L \sim 10^{33}$ cm^{-2} h^{-1} right after injection. The mean life of the beams, on the contrary, decreased with increasing E and it was typically about 10 h at $E = 1$ GeV.

The drawings of two projected views of the main apparatus are shown in Fig. 1. Additional equipment, not shown in Fig. 1, was also installed at the same straight section: *a*) a monitoring system ([8a,18]), which was used to measure continuously the machine luminosity by means of Bhabha scattering at small angles, a process which is considered to be correctly described by quantum electrodynamics since it involves small momentum transfers; *b*) a device ([19]) suitable to investigate experimentally, by a tagging technique, the reactions

$$e^+e^- \to e^+e^- + (\text{hadrons, leptons}) \tag{2}$$

which in themselves are of considerable interest ([20-22]).

The main apparatus was made up of two telescopes located on opposite sides of the straight section of the machine. From a point at the centre of the straight section, both telescopes covered nearly $\frac{1}{4}$ of the total solid angle. Each telescope was composed of scintillation counters $(E_i(I_i), i = 0, \ldots, 5)$, Čerenkov counters ($\check{C}_E$, $\check{C}_I$, see Appendix A) optical spark chambers (C_1, C_2, C_3, C_4) and lead and iron absorbers. Additional counters, A and B, were placed above and below the vacuum chamber in order to increase the solid angle for the de-

---

([15]) B. Borgia, F. Ceradini, M. Conversi, M. Grilli, A. Mulachié, L. Paoluzi, W. Scandale, P. Spillantini and R. Visentin: *Phys. Lett.*, **35** B, 340 (1971).

([16]) « Gruppo Adone » Frascati LNF-70/48 (1970); Frascati LNF-71/7 (1971), presented at the *1971 National Particle Accelerator Conference, Chicago.*

([17]) V. Alles-Borelli, M. Bernardini, D. Bollini, P. L. Brunini, E. Fiorentino, T. Massam, L. Monari, F. Palmonari and A. Zichichi: *Nuovo Cimento*, **7** A, 345 (1972).

(*) As shown in ref. ([16]) the average luminosity changed from $8 \cdot 10^{31}$ to $6 \cdot 10^{32}$ cm^{-2} h^{-1} when E increased from 0.7 to 1.2 GeV/beam.

([18]) G. Barbiellini, B. Borgia, M. Conversi and R. Santonico: *Atti Accad. Naz. Lincei*, **44**, 233 (1968).

([19]) G. Barbiellini and S. Orito: Frascati LNF-71/17 (1971).

([20]) See, also for reference to previous theoretical papers on the same subject: S. J. Brodsky, T. Kinoshita and H. Terazawa: *Phys. Rev. D*, **4**, 1532 (1971).

([21]) V. E. Balakin, A. D. Bukin, E. V. Pakhtusova, V. A. Sidorov and A. G. Khabakhpaskev: *Phys. Lett.*, **34** B, 663 (1971).

([22]) C. Bacci, R. Baldini-Celio, G. Capon, C. Mencuccini, G. P. Murtas, G. Penso, A. Reale, G. Salvini, M. Spinetti and B. Stella: *Lett. Nuovo Cimento*, **3**, 709 (1972).

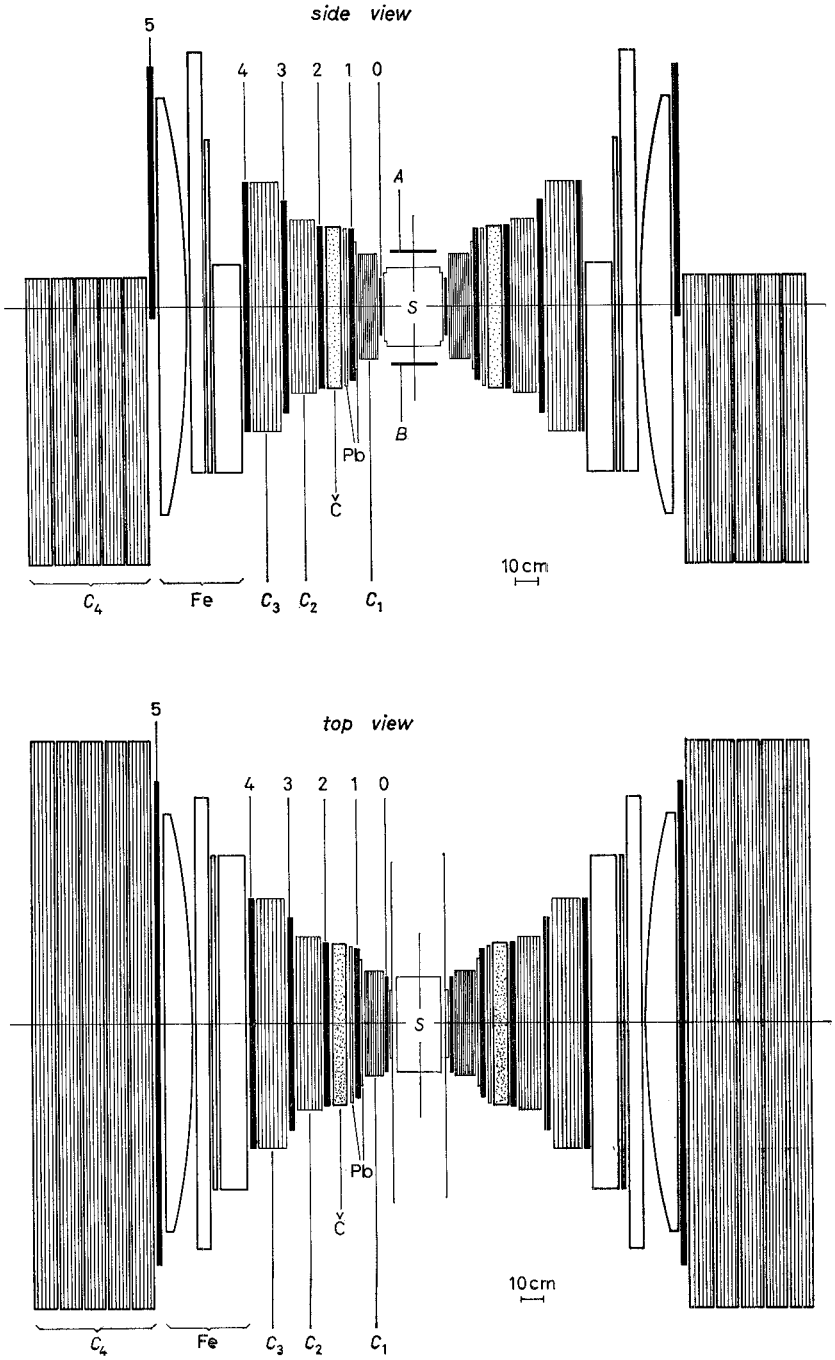

Fig. 1. – Schematic views of the apparatus. C_1 are thin-foil spark chambers used for the space reconstruction of the events. C_2, C_3 and C_4 are thick-plate spark chambers used to observe the development of electromagnetic showers and/or the interactions and stop of charged particles. Č are water Čerenkov counters. The counters numbered from 0 to 5 are scintillator counters. A and B are scintillators placed above and below the vacuum chamber to increase the solid angle for multibody events. S, the « source », is the crossing region of the bunches.

tection of multiparticle final states. They were not required, however, in the formation of the « master coincidence » (defined by eq. (3) below) which triggered the spark chambers and the camera film advance.

The optical system is briefly described in Appendix A. The two orthogonal views of the chambers, shown in Fig. 1, together with a data box containing all relevant information listed at the end of this Section, were recorded on a single 70 mm × 100 mm frame.

Figure 2 gives the sequence of thicknesses, in g/cm², of the various elements present in the telescopes (see also Table VIII and Table IX in Appendix A).

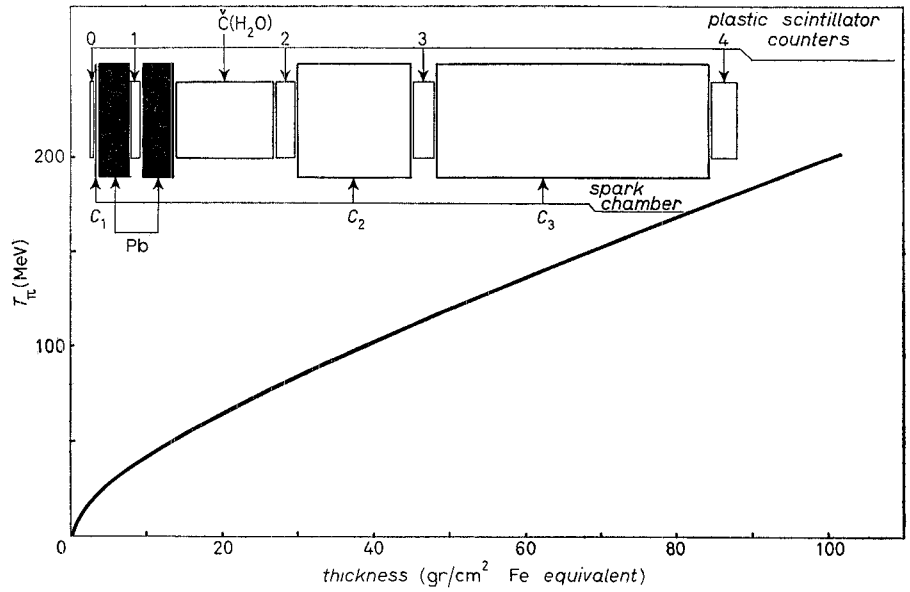

Fig. 2. – Minimum kinetic energy T_π required by a charged pion to penetrate to a given depth in a telescope. Counter 5, not shown, was placed after 380 g/cm², it corresponds to $T_\pi \sim 605$ MeV. Thicknesses of various elements are given in equivalent thicknesses of iron.

The first spark chambers C_1 are thin-foil chambers used for the spatial reconstruction of tracks. C_2 and C_3 are thick-plate spark chambers which were essential for the identification of particles by observation of their behaviour in traversing them (see Sect. **3**). The end spark chambers C_4 are also thick-plate chambers covering $\sim 50\,\%$ of the solid angle of the telescopes (*). The thickness of the iron absorber placed before chamber C_4 in each telescope was

(*) The weight of each telescope was in excess of 20 ton and for obvious practical reasons it was not feasible (nor necessary) to extend the thick plate end chambers C_4 above the horizontal median plane.

adjusted as the beam energy changed, so that muons from process $e^+e^- \to \mu^+\mu^-$ are stopped in these chambers ([23]). On the contrary, pions from $e^+e^- \to \pi^+\pi^-$, or from multihadron events, with high probability undergo nuclear interactions in the preceding absorber and essentially do not reach C_4.

The logic involved in triggering the optical spark chambers was rather complex, for two reasons. First we wanted to detect multibody events, simultaneously with the collinear events associated with two-body final states, *i.e.* e^+e^-, $\mu^+\mu^-$, $\pi^+\pi^-$, K^+K^-. Secondly, the rate of cosmic rays traversing the two telescopes was slightly in excess of one per second, far greater than that for events produced by the collisions of e^+ and e^- bunches. A strong rejection against cosmic rays was therefore needed, not only to avoid a possible source of background for the process $e^+e^- \to \mu^+\mu^-$ ([23]), but also in order to keep the triggering rate and film advance at a reasonable value of a few per minute (*).

The need to select the various types of e^+e^- events with high efficiency, combined with the necessity of an efficient rejection of cosmic rays, forced us to use two different triggers. The first was designed for the detection of the annihilation events $e^+e^- \to \mu^+\mu^-$, and the second for the detection of all the other events. The rejection of cosmic rays was based on three requirements, of which only the first was common to both triggers. These requirements were: *a*) correct timing, relative to the instant of collision of the e^+, e^- bunches, achieved by exploiting the phase of a signal (r.f.) from the machine radiofrequency; *b*) correct times of flight between the two counters 3 and between the two counters 4 of the two telescopes, the two counters of each pair being traversed simultaneously only by particles from two-body events ([24a]); *c*) absence of a signal from either of two counters 5. In order to avoid any appreciable loss of e^+e^- events, both conditions *a*) and *b*) were imposed with time windows increased by a substantial factor. More stringent time criteria subsequently were applied, however, during the analysis of the events, as all times of flight were measured and recorded in digital form on each photograph.

The trigger logic used to detect the various types of events is explained in Appendix A. In order to suppress the rate of picture taking, we were forced to use a high-order coincidence and some amount of absorber between the counters. This amount was chosen as a compromise between the need to decrease the machine background and the desire to minimize the loss of multihadron events.

([23]) B. BORGIA, F. CERADINI, M. CONVERSI, L. PAOLUZI, R. SANTONICO, G. BARBIELLINI, M. GRILLI, P. SPILLANTINI and R. VISENTIN: *Lett. Nuovo Cimento*, **3**, 115 (1972).

(*) At the occurrence of a trigger coincidence, the electronics was « paralyzed » for ~ 3 s to allow full recovery of the H.T. power supplies (Appendix A). A triggering rate of more than a few per minute would therefore result in an intolerable loss of events.

([24]) *a*) L. PAOLUZI and R. VISENTIN: *Nucl. Instr. Meth.*, **65**, 345 (1968); *b*) B. D'ETTORRE-PIAZZOLI and R. VISENTIN: Frascati report LNF 69/65 (1969).

The following 8-fold master coincidence, $M_{\text{m.h.}}$, was adopted to select multihadron events (*):

$$M_{\text{m.h.}} = E_0 I_0 E_1 I_1 E_2 I_2 (E_3 + I_3)(E_4 + I_4)(\overline{E_5 + I_5})\,\text{r.f.}, \tag{3}$$

where E_i and I_i $(i = 0, 1, 2, \ldots, 5)$ represent respectively the signals from the scintillation counters in the external and internal telescopes, as shown in Fig. 1, and r.f. is the radiofrequency phase signal from the machine as previously mentioned.

As one can see from eq. (3), the minimum penetration required for charged particles to produce the coincidence $M_{\text{m.h.}}$, is up to counter 2 of one telescope and up to counter 4 of the opposite telescope. As seen in Fig. 2 the corresponding mimimum kinetic energies for pions are 90 MeV and 185 MeV, respectively.

All spark chambers were triggered and the film was advanced on the occurrence not only of the trigger $M_{\text{m.h.}}$, but also of the other trigger $M_{\mu\mu}$. The latter trigger was used in selecting muon pairs and is described in Appendix A.

All the counters were so operated that minimum-ionizing particles traversing any part of the scintillator were recorded by the logic circuitry with an efficiency greater than 99 %. The time resolution for the master coincidences was $\sim$10 ns (half-width at half-maximum), which is small when compared with the time between two consecutive collisions of e^+e^- bunches, *i.e.* 117 ns.

In addition to the side and top views of all the spark chambers, a data box also was photographed. The following information was presented in digital form in the data box:

a) Date and time.

b) Frame number.

c) Pattern of coincident pulses from counters E_0, I_0; E_3, I_3; E_4, I_4; E_5, I_5; $\check{C}_E$, $\check{C}_I$; A and B.

d) Time between instant of a bunch-bunch collision and a pulse from either of counters 1, (called $T_{\text{1-r.f.}}$).

e) Sum of pulse heights in counters I_2 and I_3 (called H_I), and E_2 and E_3, (called H_E) ([24b]).

f) Delay times between the two counters E_3 and I_3 (called T_{33}) and between the two counters E_4 and I_4 (called T_{44}) ([24a]).

g) Counting rate of luminosity monitor, integrated from the beginning of the run until the time of the photograph.

For further details on the apparatus see Appendix A.

(*) This type of trigger was used during most of the measurements when Adone was operated in the energy interval $1.5 \leqslant 2E \leqslant 2.0$ GeV. Other master coincidences which were used to trigger spark chambers outside this interval are defined in Appendix A.

3. – Checks and calibration of the apparatus.

Due to the complexity of the apparatus previously described, it was essential to test continuously its performance using information registered on scalers, nixie lamps and multichannel analysers, as well as by making stability checks. The latter were done daily with cosmic-ray runs while Adone was not operating. Some of the typical distributions are given below.

In Fig. 3 an example of distributions of the times of flight, $T_{1\text{r.f.}}$, for cosmic rays and wide-angle Bhabha scattering (WAS events) is shown. Pulse height

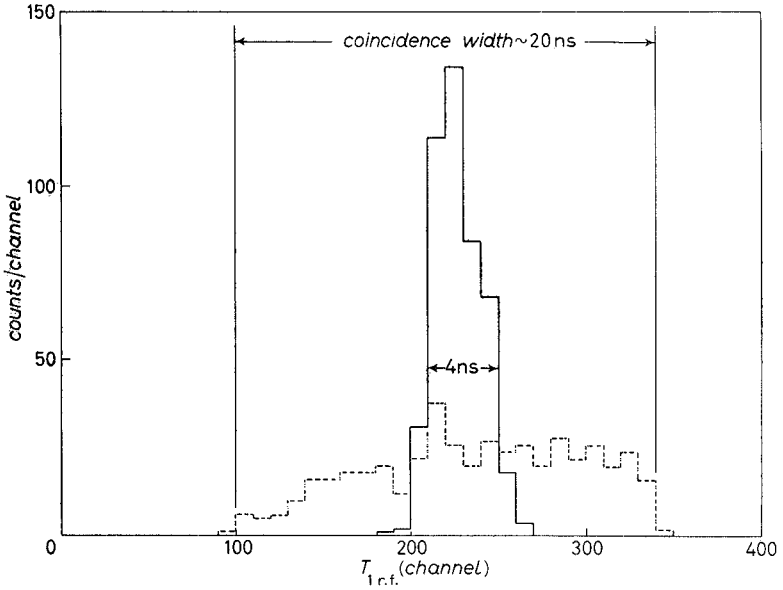

Fig. 3. – Distribution of the time of flight $T_{1\text{r.f.}}$ between either one of counters 1 and the radiofrequency phase signal, r.f., for cosmic rays and wide-angle Bhabha scattering events (WAS): ——— e^+e^- WAS, — — — cosmic rays.

distributions for counters 2 and 3 were also recorded during both machine and cosmic-ray runs. Examples of such distributions are given in Fig. 4. Similarly the time-of-flight distributions T_{33} and T_{44} were also recorded during both types of runs. These distributions were used for the interpretation of collinear events and have been discussed in previous pubblications ([15,23]).

In addition to on-line checks and calibrations, special calibration runs, already partially described elsewhere ([9a]), were made with electrons from the Frascati 1 GeV electron-synchrotron. The purpose of these runs was to determine the response of the spark chamber counter telescopes to electrons of various energies. For these tests spare spark chambers and counters identical to those

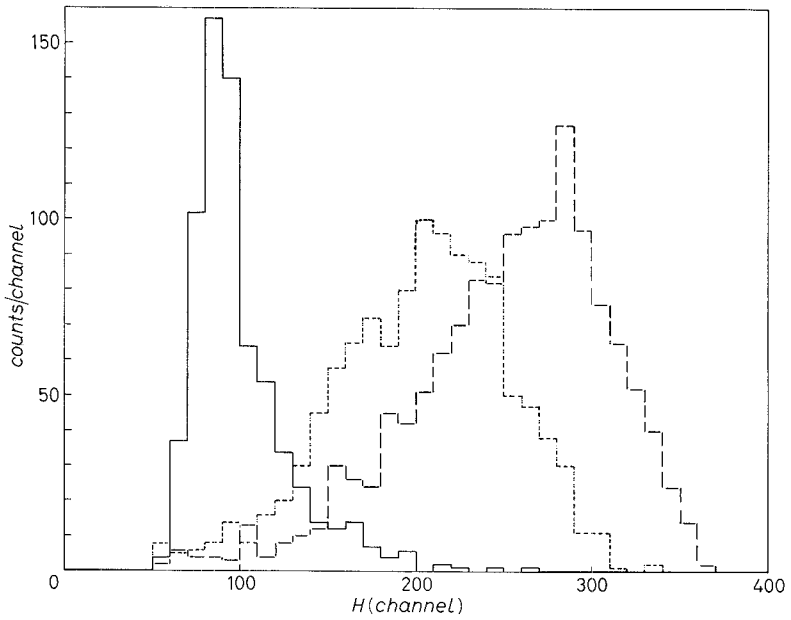

Fig. 4. – Distribution of pulse heights, $H_E(H_I)$, for cosmic rays and electrons of given energies: ——— cosmic rays, – – – electrons of 750 MeV, — — — electrons of 1050 MeV.

used in Adone were employed to set up one of the two actual telescopes up to chamber C_3. Calibration measurements were performed on it for electron energies E_e between 50 MeV and 500 MeV. The response of the telescopes to electrons of energies $E_e \geqslant 600$ MeV was obtained from WAS events recorded in the main runs carried out at Adone, so that there was no need for special calibration measurements at these higher energies.

The probabilities P_2 and P_3 that an electron give a signal, respectively, in counters 2 and in both counters 2 and 3 of the apparatus, were determined for each energy value. These probabilities are reported in Fig. 5 as a function of the energy E_e. A first conclusion resulting from these measurements is that electrons of energy below $(200 \div 250)$ MeV have but a small probability of triggering the apparatus through the master coincidence, $M_{\text{m.h.}}$, defined in Sect. **2**.

In order to observe in a statistically significant way the behaviour of the electrons in the shower chambers C_2 and C_3, a total of about 1000 pictures were taken. The analysis of these photographs was rather detailed since the criteria derived from it allowed us to distinguish electrons from hadrons in the observed multiparticle events.

In the analysis of spark-chamber pictures the following definitions were introduced: *a*) a group of n non-aligned sparks appearing in more than two

gaps and within an angle of 15° from the primary electron, was called a *shower*; *b*) n sparks aligned along the primary-electron direction was called a *single track*. It should be noted, however, that for $n < 3$, it was not found possible to distinguish between a shower and a single track.

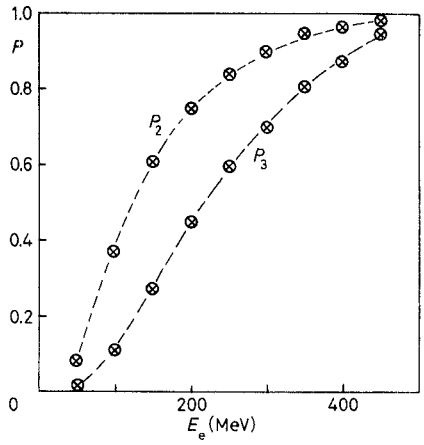

Fig. 5. – The probabilities for an electron to produce a pulse in counter 2, P_2, and in both counters 2 and 3, P_3, as a function of electron energy, E_e.

Also in this analysis the events were divided into two categories: i) events with a coincident pulse in counter 2 but none in counter 3, and ii) events with coincident pulses in both counters 2 and 3. The probabilities for the occurrence of i) and ii) were indicated previously as P_2 and P_3, respectively.

Category i). The fraction of events of this type that have less than 3 sparks ($n < 3$) appearing in the spark chamber C_2 is given in Fig. 6 as a function

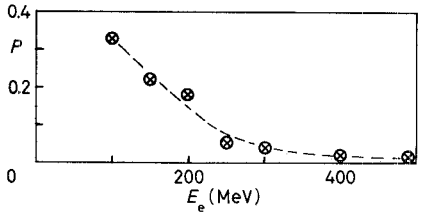

Fig. 6. – The probability for an electron to give a pulse in counter 2 and not in counter 3 and to produce less than 3 sparks in spark chamber C_2 as a function of electron energy, E_e.

of electron energy E_e. About 5% of the electrons in this category at all energies produce single tracks with $n \geqslant 3$ in C_2. The remaining events give rise to showers with $n \geqslant 3$, as defined above.

Category ii). This category presents fewer difficulties in the event classification than category i) as both spark chambers C_2 and C_3 are considered and, consequently, on the average there are more sparks to be utilized in the analysis. The average number of sparks in showers produced by electrons in chambers C_2 and C_3 as a function of electron energy is given in Fig. 7. In the same Figure the fluctuation in this number about the average also is indicated by maximum and minimum curves. On the basis of these results, the minimum number of sparks to be used in identifying showers was set at four, *i.e.* $n \geqslant 4$.

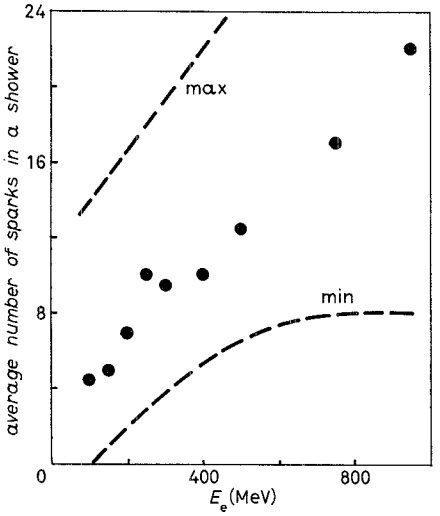

Fig. 7.

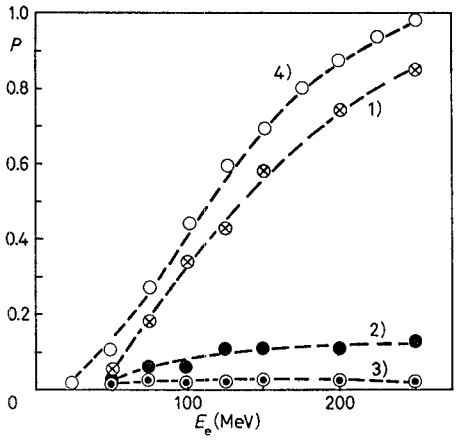

Fig. 8.

Fig. 7. – Average number of sparks in showers appearing in chambers C_2 and C_3 per electron of energy E_e which has produced a pulse in counters 2 and 3. The maximum and minimum limits also are given.

Fig. 8. – The probabilities that an electron of energy E_e produce a pulse in counters 2 and 3 and: 1) produce a shower with at least 4 sparks, 2) produce a single track with at least 4 aligned sparks and 3) produce an ambiguous grouping of sparks or a number of sparks less than 4. The curve 4) is the sum of curves 1), 2) and 3) and represents the probability P_3 that an electron of energy E_e give a pulse in both counters 2) and 3) (see Fig. 5).

The results of an analysis of events of category ii) are presented in Fig. 8. Curve 1) gives the probability that an electron produce a shower ($n \geqslant 4$), curve 2) a single track, and curve 3) an ambiguous result. Curve 4) is the sum of curves 1), 2), and 3) and is the probability P_3 (of Fig. 5) that an electron produce signals in counters 2 and 3. Thus, for those events in which counters 2 and 3 are required in the trigger, the probabilities per incident electron are given in this Figure for the different spark configurations at each energy E_e.

By using a more restrictive definition for a single track, *i.e.* requiring $n \geqslant 6$, a greater certainty in particle identification is possible. This can be seen in Fig. 9, where the probability that an electron give a pulse in counters 2 and 3 and produce a single track with $n \geqslant 6$ is presented.

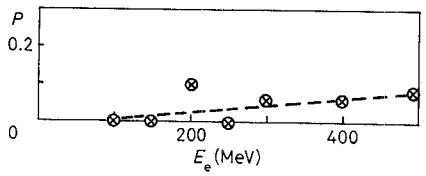

Fig. 9. – The probability that an electron of energy E_e give a pulse in counters 2 and 3 and produce in chambers C_2 and C_3 a single track with at least 6 aligned sparks.

The results discussed in this Section furnish the basis for particle identification throughout this paper.

4. – Scanning and event selection.

Scanning for events was carried out on projected images of the film enlarged to a size corresponding to ~ 0.2 of the actual one. During the scanning, events were selected by requiring that the associated tracks appear to come from a common point in the e^+e^- interaction region. Tracks in the thin-plate spark chambers C_1, when extended, should come from a common origin within ± 0.5 cm perpendicular to the beam and ± 1 cm along the beam direction. Furthermore, it was required that the reconstructed vertex of the event coincide, within ± 1.5 cm, with the beam centre in the front view. These limits were set taking into account the average precision in the spatial reconstruction of the events, and the multiple Coulomb scattering of the particles along their paths. Of course some e^+e^- events may have been lost on the application of these geometrical criteria. The loss, however, was small, being $\sim 2\,\%$ for events having three or more charged particles within the solid angle of the apparatus (*).

(*) Even though it is not essential for the analysis of multihadron events, mention should be made of the fact that for each event selected in the film scanning, the information from the « DATA BOX » (see Sect. **2**), as well as supplementary information relevant for the subsequent analysis, was transferred to computer cards. This supplementary information included: 1) collinearity condition for two-track events; 2) number of tracks, converging to a common point in the e^+e^- interaction region, for multitrack events; 3) behaviour of the detected particles in the thick-plate spark chambers C_2 and C_3 (« single track », « shower »—see Sect. **3**); 4) presence of correlated tracks and possible stops in the end chambers C_4.

Selected events were then classified in the following categories:

a) two-track collinear events if the tracks were collinear within 10° in both views of the apparatus;

b) two-track noncollinear events, hereafter called $2C$ events, if the collinearity angle between the tracks was $> 10°$ in at least one view;

c) events with more than two charged particles detected by the apparatus, *i.e.* $3C$, $4C$ and $5C$ events.

Two-track collinear events (class *a*)) can be attributed to the following processes:

i) Wide-angle e^+e^- elastic scattering (WAS events). These events occurred at a rate of about 20 per hour, with Adone operating at $E = 1$ GeV and $L \approx 10^{33}$ cm^{-2} h^{-1}. They were readily identified by the electromagnetic shower produced along each track in the spark chambers C_2 and/or C_3 ([15]). Also, as seen in Fig. 4, a large pulse height in counters 2 and 3 of both telescopes was usually observed. In the present analysis the number of these events was used as a monitor, from which the absolute cross-sections for multihadron production was then deduced. These WAS events served also to determine the frequency distributions of T_{33}, T_{44} and $T_{\text{tr.f.}}$ for e^+e^- collision events and thereby to set fiducial limits for these three times of flight to ensure the selection of the events due to e^+e^- collisions.

ii) Muon-pair production: $e^+e^- \to \mu^+\mu^-$ ([23]). These events occurred at a rate of ~ 1/h for $E = 1$ GeV and $L \approx 10^{33}$ cm^{-2} h^{-1}.

Some results on the above electromagnetic two-body processes i) and ii) have been previously published ([15,23]).

iii) Hadron-pair production. These events were mostly of the type $e^+e^- \to \pi^+\pi^-$. We have also observed, however, one unambiguous case of K^+K^- pair production event, as reported at the Cornell Conference ([6a]). The results on these hadronic two-body processes will be discussed elsewhere ([7b]).

Most of the events belonging to class *b*) were WAS events which had suffered some radiation loss in the initial state (*). Almost all these events appear as coplanar with the beam direction, but not collinear ([17]). Class *b*) includes, of course, some multibody final states from e^+e^- interactions, as well as events produced by the interaction of the circulating beam with the gas in the straight section of Adone. This background will be discussed in the following Section.

Finally, the multibody events of class *c*) mostly are events in which only

(*) Events with final-state radiation losses are also present in category *b*), but they are infrequent, since they require the improbable emission of a hard photon.

hadrons are produced. The analysis of this category of events is the principal subject of this paper.

For the selected events belonging to categories *b*) and *c*) drawings were made for the two orthogonal views of each event. All details useful for the further analysis of these events (*e.g.* large-angle scattering, stopping points, nuclear interactions, etc.) were recorded in these drawings.

5. – Background events.

During the operation of Adone the pressure of the residual gas in the vacuum chamber was usually about 10^{-9} Torr. Part of the machine background therefore was due directly to the interactions of the beams with this residual gas. Additional background events were produced by beam losses and subsequent collisions against the walls of the vacuum chamber. These last-mentioned background events could be easily recognized by attempting to reconstruct their origins from the corresponding pictures. On the contrary, the former background events could not be distinguished from e^+e^- events because the observed beam-gas collisions occur along the beam and thus in the e^+e^- interaction region as well. The separation between e^+e^- and spurious events of the former type, therefore, had to be done on a statistical basis. For this purpose, special background runs were interspersed between main runs, at various beam energies. As shall be seen, the contribution of spurious events is appreciable only for the events classified as category *b*) in the previous Section.

The determination of the frequency and types of spurious events was based mostly on background runs in which the machine was operated with a single high-current beam (typically (40÷60) mA). As a further check, background runs also were made in which Adone operated with both e^+ and e^- beams, but with the beam trajectories spatially separated by a few mm so as to eliminate collisions between e^+ and e^- bunches. The events observed in all the background runs were studied with the aim of setting criteria that hopefully would improve the signal-to-noise ratio for the multihadron events produced in e^+e^- collisions.

The normalization between the background runs and the e^+-e^- colliding beam runs was based on measurements of small-angle electron (or positron) scattering on residual gas nuclei. These measurements were made in both types of runs by using the small-angle scattering luminosity monitor ([18]), a drawing of which is shown in Fig. 10. Each of the four telescopes $P_iG_iS_i$ is made up of two scintillation counters, P_i, G_i, and a shower counter S_i. These telescopes are located in such a way as to detect electrons scattered at angles from 3.5° to 6.1°, when measured from the centre of the colliding region. The shower counter S_i was operated to select high-energy electrons, with energy comparable to that of the beam, and to reject lower-energy background electrons.

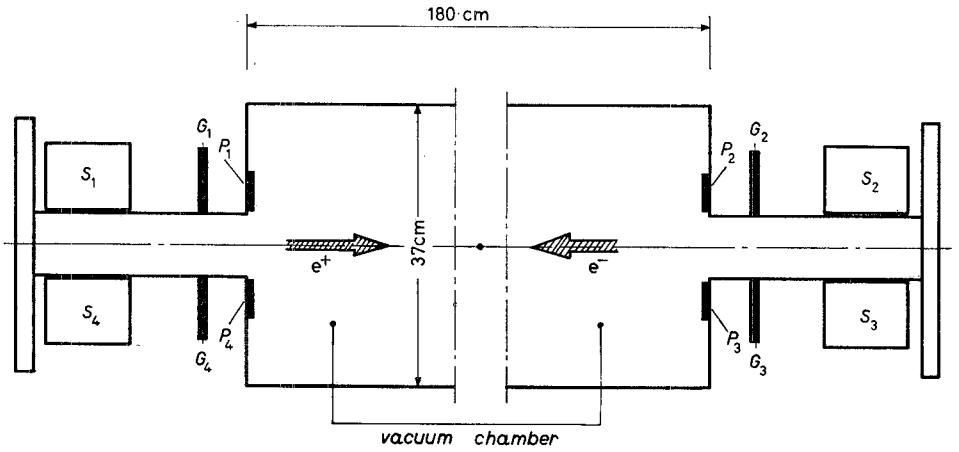

Fig. 10. – Monitoring set-up for the luminosity measurement. P_i, G_i ($i = 1, 2, 3, 4$) are scintillation counters; S_i are shower counters.

Small-angle electron (or positron)-gas scatterings were detected by the threefold coincidences $T_i = P_i G_i S_i$, where $i = 1, 4$ for electrons and $i = 2, 3$ for positrons.

The following checks were carried out to make sure that the T_i coincidences were essentially due to small-angle e^- (or e^+) scattering on residual gas nuclei:

i) T_i was found to be a linear function of both, circulating current and residual gas pressure, as expected for events produced by beam-gas interactions;

ii) with only one e^- circulating beam it was found that $T_{1,4} \gg T_{2,3}$, as expected for small-angle scattering of e^- on nuclei. The reverse (*i.e.* $T_{2,3} \gg T_{1,4}$) was found to be true when only one e^+ beam was circulating.

Furthermore, when Adone was operated with two colliding beams as in the main runs, 99.8 % of the counting rates from a single arm of our monitoring system, T_i, were found to be due to beam-gas interactions. Therefore these threefold coincidence rates were used for the normalization between the main and the background runs.

Background runs were carried out at total energies of 1.5 GeV, 1.9 GeV and 2.1 GeV. On the basis of the normalization procedure outlined above, they were equivalent to ~ 40 %, ~ 50 % and ~ 75 %, respectively, of the corresponding colliding beam runs. No multibody events of the types $3C$, $4C$, $5C$ were observed at any energy; $2C$ events instead were observed at a rate depending upon the required penetration depth of secondary particles in each telescope. The trigger employed, $M_{\text{m.h.}}$, (see Sect. 2) implied that at least one particle penetrated to counter 4. The rate of background events depended

then on the penetration of the other particle in the opposite telescope as indicated in Table I.

TABLE I. – *Background events.*

$2E$ (GeV)	Number of $2C$ events	
	minimum penetration to counter 2	minimum penetration to counter 3
1.5	5	0
1.9	7	1
2.1	22	9

It is seen from Table I that, in order to reduce substantially the number of background events, it is convenient to retain only those $2C$ events in which both particles penetrate to counters 3. Mention should also be made of the fact that a rather large fraction, $\sim 30\,\%$, of the background events listed in Table I contains shower-producing electrons.

Of course, since no background event of the types $3C$, $4C$, or $5C$ was observed, the requirement of penetration to counter 3, adopted in the analysis of the $2C$ events, was no longer applied to events with higher visible multiplicity.

6. – Phenomenological classification of events.

We recall from Sect. 4 that an nC event is a phenomenological classification indicating that n charged particles emanated from a point in the e^+e^- interaction region and were detected by the two telescopes of the apparatus. These events are now to be classified in a more detailed way taking advantage of the calibration measurements discussed in Sect. 3 and the background measurements reported in the previous Section. This allows the possible contamination of spurious events to be removed from the multihadron sample.

As a general requirement, all the multibody events had to coincide in space and in time with the collision of the two e^+ and e^- bunches. More precisely, it was required, first, that the tracks of any event have their common origin within a fiducial region coinciding with the interaction region. Moreover the event had to occur within a fiducial time region around the instant of beam-beam collision. Both these two fiducial regions were established on the basis of the two corresponding distributions for WAS events, as outlined in Sect. 4, point i).

The analysis which follows will be made separately for the $2C$ events, for $3C$ events, and for $4C$ and $5C$ events.

6·1. *2C-event classification.* – Based on the results of the previous Sections, a $2C$ event is defined as an event with only two charged nonaligned tracks, one of which penetrated to counter 4 and the other at least to counter 3 in the opposite telescope. In addition to the two general requirements specified above, it was also required that the time interval T_{33} between the pulses in the two counters 3 be consistent with that obtained for WAS events. Such a consistency is satisfactorily exhibited in the two distributions plotted in Fig. 11.

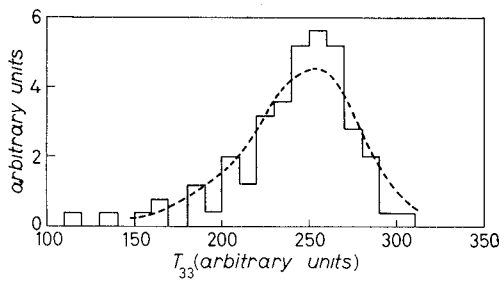

Fig. 11. – Distribution of the time of flight T_{33} between the counters E_3 and I_3, for $2C$ events. The analogous distribution for e^+e^- WAS events is given for comparison (— — —).

In order to accept a $2C$ event as a candidate for having been produced in reaction (1), the following criteria were adopted during the analysis. One particle of each $2C$ event was required:

i) To have penetrated to counter 4.

ii) To have given no indication of shower production in either chamber C_2 or C_3.

iii) To have at least 6 aligned sparks along its track, which on the average contained the same number of sparks as the tracks of cosmic-ray muons. As seen from Fig. 12 this average number is ~ 11. A track with these characteristics will be called a «long track» and indicated by T_L.

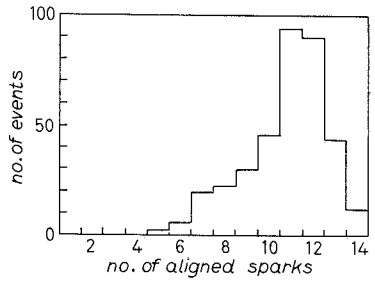

Fig. 12. – Frequency distribution of aligned sparks in a penetrating non-interacting hadron track (T_L), from $2C$ events.

iv) The pulse height H_E (H_I), defined in Sect. **2**, should be smaller than ~ 1.5 times the value corresponding to a minimum-ionizing particle.

The pulse height distribution obtained for a sample of T_L tracks is shown in Fig. 13. One sees from this Figure that most of the T_L tracks correspond to minimum-ionizing particles.

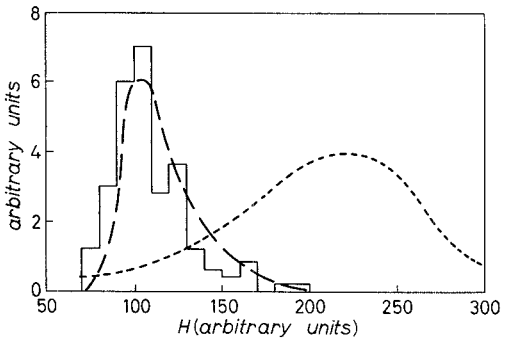

Fig. 13. – Distribution of pulse heights, H_E (H_I), for penetrating hadronic tracks in $2C$ events compared with cosmic-ray and electron distributions: ——— cosmic rays, – – – electrons (WAS events).

Once a T_L track had been observed in one of the two telescopes, the following possibilities were considered for the behaviour of the other particle, in the thick-plate chambers of the opposite telescope:

a) The particle gave a T_L track.

b) The particle produced a single but shorter track (T_S) ending before counter 4. In this case the presence of at least 4 aligned sparks was required in order to define its single track behaviour.

c) The particle produced a well-identified electromagnetic shower as defined in Sect. **3**. This case will be indicated in what follows by S.

d) The particle had a behaviour which did not allow unambiguous classification in either category T or S. This case will be indicated by X.

The two possibilities *a*) and *b*) were combined together to define the single-track behaviour indicated, in the following, by $T = T_L$ or T_S.

The numbers of observed events having a T_L track in one telescope and either T, S, or X behaviour in the opposite telescope, *i.e.* the numbers with configurations T_L/T, T_L/S and T_L/X, are given in Table II. The data obtained in background runs and normalized as explained in Sect. **5** are also reported in the same Table. The last column of the Table contains the numbers of associated WAS events.

TABLE II. – *Observed configurations in 2C events.*

$2E$ (GeV)	Type of measurement	Number of 2C events			Number of WAS events
		T_L/T	T_L/S	T_L/X	
1.2	e^+e^-	9	0	0	760
	background	not measured			
1.5	e^+e^-	33	3	2	2419
	background	0	0	0	
1.9	e^+e^-	42	4	2	2112
	background	0	2 ± 2	0	
2.1	e^+e^-	86	12	7	3415
	background	3 ± 2	7 ± 4	3 ± 2	

One notes that the configurations T_L/S and T_L/X are mainly the result of beam-gas interactions. Also it is seen that the ratio S/X is ~ 2. Considering the results of the calibration measurements reported in Fig. 8, one concludes that the S and X behaviours are very probably due to low-energy electrons. At the present statistical level of this experiment it seems reasonable to assume that all T_L/S and T_L/X events are due to beam-gas interactions.

The fraction of the T_L/T configurations in which one or both tracks are due to electrons can be estimated as follows. The two main nonhadronic processes which might simulate these configurations are:

i) Electron-gas scattering. From the numbers of T/S configurations and the probabilities that an electron simulate a T track, as given in Fig. 7, we find that out of the 86 events observed at $2E = 2.1$ GeV (Table II), only ~ 2 events should be due to this background process.

ii) e^+e^- scattering (WAS) events, with an angle of noncollinearity in excess of 10°. Only 7% of all WAS events have noncollinearity angles $> 10°$ and with the probability of $\sim 0.1\%$ that both electrons would appear as T and T_L tracks (Sect. **3**), one finds that ~ 0.5 events is the expected contribution to the observed T_L/T configurations. Such a contribution will be neglected.

The above discussion shows that the bulk of the T_L/T events cannot be made up of electrons. Evidence for their hadronic nature will be given in the subsequent Section in which nuclear interactions in the material of the telescopes are considered. In the discussion that follows T_L/T events will be called $2T$ events.

6·2. *3C-event classification.* – We recall that the master coincidence, $M_{\text{m.h.}}$, implied the penetration of at least one particle up to counter 4 of one telescope,

and up to counter 2 for a particle in the opposite telescope. Thus every multibody event contained at least one «long track» T_L (Sect. 6·1) and at least one track reaching counter 2 of the opposite telescope.

A total of 266 $3C$ events were observed in the e^+e^- collisions at all energies. However no $3C$ event was observed during background runs with a single beam or two noncolliding beams. The great majority of these events, 245, contained two single tracks, one of which was a T'_L track. Twenty of the remaining events had characteristically only one clear single track (usually a T_L track) and in one event three showers were observed. These latter 21 events will not be considered further in this paper.

It is important to estimate the fraction of $3C$ events containing electrons and, therefore, not due to the multihadron reaction (1). This estimate has been made starting from the seven T_LTS events in which one shower was observed. Using the results of the calibration measurements reported in Fig. 8 and assuming pessimistically that all the observed showers are produced by 100 MeV electrons, we found that the above fraction is only about 1% of the $3C$ events. This percentage is an over-estimate, since some of the events with showers may well be due to pion charge exchange. The very small number of electrons as final-state particles is also consistent with the observations on pulse height in counters 2 and 3, when only one particle is seen to traverse them in a telescope. This pulse height distribution results to be very similar to that for cosmic-ray muons and not for electrons.

The number of $3C$ events of the type $T_LTT(\equiv 3T)$ observed at each total energy, $2E$, is given in Table III.

TABLE III. – *Summary of results on events with more-than-two charged particles.*

$2E$ (GeV)	WAS events	$3T$	$4T$	$5T$
1.2	760	3	0	0
1.5	2419	38	14	1
1.65	992	17	8	0
1.9	2164	35	10	1
2.1	6187	122	39	6
2.4	1101	23	13	4

6·3. *$4C$- and $5C$-event classification.* – During the search for multihadron events no event having more than 5 charged secondaries was observed.

As no $4C$ or $5C$ event was observed during the background runs, all the observed e^+e^- events were included in this sample.

In analysing these events, no secondaries were seen to appear as showers. Considering the results on $3C$ events and the smaller numbers of $4C$ and $5C$ events, we have taken all the secondaries to be hadrons. The number of the

events, which have been called $4T$ and $5T$, observed at the various total energies $2E$, are given in Table III.

6·4. *Auxiliary observations on multiparticle events.* – Electromagnetic showers produced by photons also were observed in multibody events by their conversion before or in chambers C_2 and C_3. These showers were not associated with charged particles of the event, as specified by the requirement (Sect. **3**) of observing the nonaligned sparks within a 15° cone around each track direction. In most cases the direction of the photon could only be roughly established by the observation of the shower produced. As no such shower was observed among events of the type $e^+e^- \to \mu^+\mu^-$ or from cosmic-ray runs, the photon conversions observed in multihadron events have been assumed to come from the decays of neutral pions produced in these events.

In some cases showers also were observed in chambers C_1. They presumably originated in the wall of the vacuum chamber of the machine. These showers could have been produced by secondary electrons, however we recall that the number of secondary electrons, particularly in $3C$, $4C$ and $5C$ events, is very small ($< 1\%$ of all tracks in $3C$ events). Consequently, all the showers observed in chambers C_1 associated with multiparticle events, were attributed to photons from π^0 decay.

Additional information concerning multibody events was given by counters A and B. The pulses from these counters were in fact recorded in the data box mentioned in Sect. **2** when they occurred in coincidence with the master trigger $M_{\text{m.h.}}$.

A summary of the numbers of events with associated γ and/or coincident pulses from counters A and/or B is given in Table IV for the different multihadronic events $2T$, $3T$, $4T$ observed at various energies, $2E$.

It was found that in $(2 \div 3)\%$ of the cases, collinear WAS events were accompanied by spurious signals in either counters A or B. Accordingly,

TABLE IV. – *Events with an associated γ and/or coincident signals in counters A and B* (a)

Total energy $2E$ (GeV)	Number of WAS events	Number of events of the type					
		$2T+\gamma$	$2T+A$ or B	$3T+\gamma$	$3T+A$ or B	$4T+\gamma$	$4T+A$ or B
1.2	760	0	0	0	0	0	0
1.5	2419	4	7	8	9	1	0
1.9	2164	15	7	11	12	1	0
2.1	6187	14	22	30	28	2	11
2.4	1101	—	—	8	5	3	1

(a) A small fraction of the events reported in this Table contained indeed more than one γ and/or signals from both counters A and B.

the numbers of events with A or B signals reported in Table IV were corrected for this small background contamination.

The usefulness of the supplementary information related to the presence of γ and/or A, B signals in the recorded events, will be made clear in Sect. **10**.

7. – The nature of secondary particles and reactions.

The criteria adopted in the selection of events as described in the previous Section ensured that secondary particles were singly charged and penetrating, and were improbably electrons. Qualitatively these particles also were seen to give rise to nuclear interactions and wide-angle scatterings. The effective experimental interaction length for nuclear interactions was estimated by determining the fraction of secondary particles from multibody events which did interact in the telescopes.

In order to compare our results with those from counter experiments on pion-nucleus interactions, an interaction was defined as the interruption of a track, without secondary tracks, or with all penetrating secondaries having angular deviations of more than 25°. Thus, wide-angle scatterings ($> 25°$) also were included as interactions. Averaging over the apparatus, the experimental absorption length in iron for the secondary particles from multiparticle events was found to be (114 ± 12) g/cm^2. This value is ~ 1.2 times the geometric interaction length for iron and is in good agreement with experimental values measured in counter experiments ([25]), when averaged over the assumed pion energy spectrum (*).

Moreover for $2T$ events, where the statistics are sufficiently high to make a more detailed comparison possible, the distribution of the interactions as a function of absorber depth is compared with other similar spark chamber results ([26]) in Fig. 14. The latter were obtained with 400, 500 and 600 MeV/c pions incident on iron-plate spark chambers. The agreement between these distributions is considered satisfactory also on account of the extended pion energy spectrum and the slight differences in the criteria followed in identifying interactions.

The above results show that the secondaries of the observed multiparticle events are mostly hadrons, with nuclear interaction characteristics consistent with those observed for pions having a kinetic energy of ~ 350 MeV. This conclusion is in line with and reinforces the conclusions of Subsect. **6**·1 and **6**·2, that most of the final-state particles in multiparticle events are not electrons. It will be assumed in what follows that all the multihadron events se-

---

([25]) A summary of these data can be found in H. OGREN: Frascati LNF-71/89 (1971).

(*) This spectrum was obtained from the Monte Carlo simulation of the experiment, which is described in Sect. **8**.

([26]) J. E. AUGUSTIN, P. MARIN and F. RUMPF: *Nucl. Instr. Meth.*, **36**, 213 (1965).

lected according to the criteria discussed in Sect. **6** and reported in the Tables II, III and IV, contain only pions in their final states. This assumption is supported

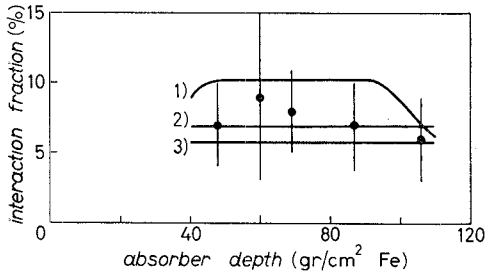

Fig. 14. – Distribution of nuclear interactions in $2T$ events as a function of absorber depth. Calibration curves from ref. ([26]) are indicated for 3 different pion momenta: 1) $P_\pi = 400$ MeV/c, 2) $P_\pi = 500$ MeV, 3) $P_\pi = 600$ MeV/c.

by the results from $p\bar{p}$ annihilations, which also have a centre-of-mass energy of ~ 2 GeV and which are recorded as having $\sim 95\,\%$ of final states with only pions ([27]). Further suggestions along these same lines are given by the low K/π ratio found in high-energy hadronic interactions ([28]).

Charged-pion production infers of course also the production of neutral pions. Analysis based on Monte Carlo estimates of the number of converted gamma-rays for event types $2T$, $3T$ and $4T$, when compared with experiment (see Table IV) indicates that the average numbers of π^0 produced is ~ 2 in each reaction.

Based on these observations, the following reactions have been considered as the major contributors to the multiparticle events reported here:

$$
\begin{aligned}
&(4) && e^+e^- \to \pi^+\pi^-\pi^0\,,\\
&(5) && e^+e^- \to \pi^+\pi^-\pi^0\pi^0\,,\\
&(6) && e^+e^- \to \pi^+\pi^-\pi^+\pi^-\,,\\
&(7) && e^+e^- \to \pi^+\pi^-\pi^+\pi^-\pi^0\,,\\
&(8) && e^+e^- \to \pi^+\pi^-\pi^0\pi^0\pi^0\,,\\
&(9) && e^+e^- \to \pi^+\pi^-\pi^+\pi^-\pi^0\pi^0\,,\\
&(10) && e^+e^- \to \pi^+\pi^-\pi^+\pi^-\pi^+\pi^-\,.
\end{aligned}
$$

([27]) C. Baltay, P. Franzini, G. Lütjens, J. C. Severtens, D. Tycho and D. Zanello: *Phys. Rev.*, **145**, 1103 (1966).

([28]) See, for instance: E. Lillethun: *Proceedings of the International Conference on Elementary Particles* (Lund, 1969), p. 165; M. G. Albrow, D. P. Barber, A. Bogaerts, B. Bosnjakovic, J. R. Brooks, A. B. Clegg, F. C. Erne, C. N. P. Gee, A. D. Kanaris A. Lacourt, D. H. Locke, P. G. Murphy, A. Rudge, J. C. Sens and F. van der Veen: *Phys. Lett.*, **40** B, 136 (1972).

The limit of six pions in the final state is a reasonable hypothesis since the fraction of $p\bar{p}$ interactions at rest with more than six pions is $\leqslant 10\,\%$ ([27]), and since, as pointed out previously, the average number of π^0's produced is $\leqslant 2$, even for $4T$ events. Also the cross-section deduced using a Monte Carlo simulation with the above reactions, results in a falling cross-section with increasing number of pions in the final state (see Fig. 25 later). Finally, it should be noticed that, if multiplicities higher than a maximum value of 6 were introduced in the analysis, the information on the reactions involved would become less significant, for with the same data the results would be less constrained due to the greater number of channels. Thus ignoring the rather small contributions from multiplicity states higher than 6 introduces less uncertainties in the resulting partial cross-sections than including them.

8. – Monte Carlo simulation of the experiment.

A Monte Carlo program was written to simulate the experiment and to calculate the efficiencies for the detection of final states with more than two charged particles. In these calculations particles were generated according to phase space and according to the reactions listed in the previous Section. Events for a particular final state were randomly generated along the beam line, with a distribution which took into account the finite length of the source. The secondary charged particles and gammas from the π^0 decay were then traced through the vacuum chamber wall and through the spark chambers and counters of the apparatus.

From these calculations the following information was obtained:

i) the efficiency for the detection of a given final state;

ii) the frequency of detected events with a pulse in counter A or B, due to a charged particle or to a γ from π^0 decay converted in the wall of the vacuum chamber;

iii) the frequency of electromagnetic showers produced by neutral pions associated with detected events.

In the calculations of the detection efficiency, the nuclear interactions of pions were taken into account by using the results of attenuation measurements in various materials as reported by different authors ([25]). The attenuation cross-section used in the computations is shown in Fig. 15 (*). These cross-sections are for pion-nucleus (Fe) collisions in which a penetrating secondary is scattered at an angle greater than 25°. For materials other than iron their

(*) Details can be found in ref. ([25]).

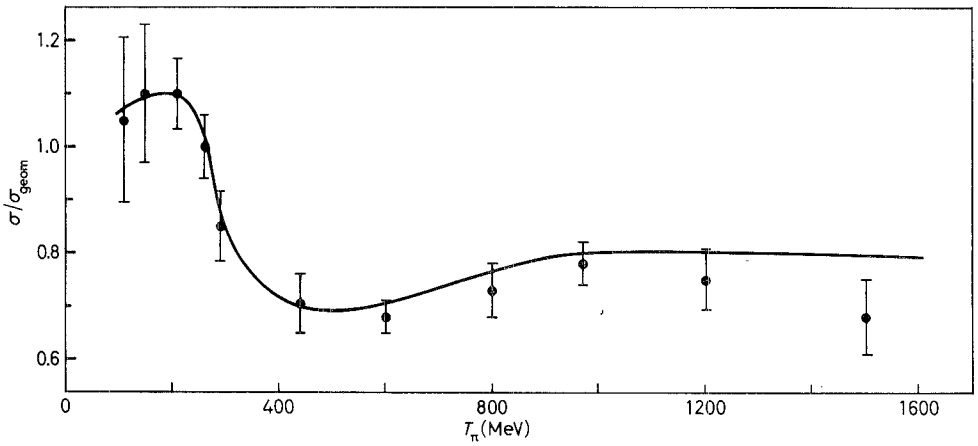

Fig. 15. – Nuclear-attenuation cross-section in iron as a function of the pion kinetic energy, T_π. These results were used in the Monte Carlo simulation of the experiment.

cross-sections were scaled by $A^{\frac{2}{3}}$. No account was taken of small effects such as π-μ decay or multiple Coulomb scattering.

For each gamma-ray from the π^0 decay, the conversion point along the direction of motion in the apparatus was randomly selected along an exponential, measured in conversion lengths. The asymptotic value of the conversion length at high energy was used. After conversion, the shower was followed as if it were a single particle, for a depth corresponding to the average penetration of a shower of that energy. The penetration as a function of energy was deduced using the results of the calibration measurements reported in Sect. **2**, as well as results by other authors ([29]).

Dynamic factors for each event were used only in the generation of three-body final states ($\pi^+\pi^-\pi^0$). The factor used was $\sin^2\Theta \sin^2\theta$ ([1]) where θ is the angle between the e^+e^- beam direction and the normal to the production plane, and Θ is the angle between the two charged pions in that plane.

The values obtained for the detection efficiencies are in the range of $\sim(1\div 7)\%$ and vary with the reaction, detection configuration, and total energy $2E$. These are shown for the most probable configurations in Fig. 16. Low values of the efficiencies are found essentially because of the relatively small solid angle of the two telescopes ($\Omega/4\pi \approx 0.2$) and because of the losses due to nuclear or range absorption of the produced pions.

The errors in the efficiencies are between 10 and 20 % for most reactions and are due principally to the statistical accuracy in the computation (*). For

([29]) R. KAJIKAWA: *Journ. Phys. Soc.*, **18**, 1365 (1963); H. THOM: *Phys. Rev.*, **136**, B 447 (1964); Z. S. STRUGALSKI: JINR Dubna report E 13-5152 (1970).

(*) For every reaction (4)-(10) about $2\cdot10^4$ events were randomly generated.

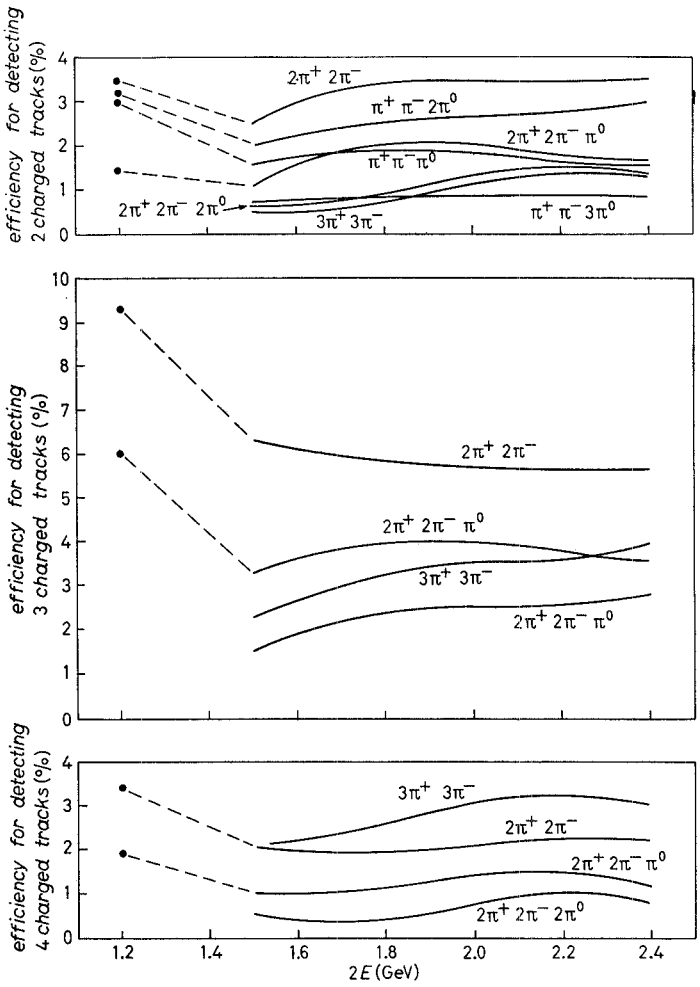

Fig. 16. – Efficiencies in various configurations for detection of processes with different final states, *vs.* $2E$. The efficiencies have been computed taking into account only invariant phase space. The values at $2E = 1.2$ GeV are for a different triggering condition.

those reactions with lower efficiencies ($\sim 1\,\%$) the error increases to $\sim 30\,\%$.

The sensitivity of the calculated efficiencies, ε, to changes in the mean free path λ_c has been estimated to be approximately equal, *i.e.*

$$\Delta\varepsilon/\varepsilon = \sim \Delta\lambda_c/\lambda_c .$$

As stated before, a statistical production mechanism was assumed in all quoted calculations. The results that would be obtained by assuming

different production mechanisms, *e.g.* $e^+e^- \to A_1^{\pm}\pi^{\mp} \to 2\pi^+ + 2\pi^-$; $e^+e^- \to \rho^0\varepsilon^0 \to$ $\to 2\pi^+ + 2\pi^-$; $e^+e^- \to \rho^0\pi^+\pi^-$, etc., will be discussed elsewhere ([30]).

9. – The reaction $e^+e^- \to \pi^+\pi^-\pi^+\pi^-$ from analysis of $4T$ events.

From the events classified as $4T$, it is possible by the procedure discussed below, to determine the number of those containing only four charged hadrons. As indicated earlier (Sect. **7**), we will assume that all secondaries are pions, *i.e.* that these special $4T$ events belong to the reaction

$$e^+e^- \to \pi^+\pi^-\pi^+\pi^- . \tag{6}$$

Of course $4T$ events of this type were searched for among those which had no associated γ (Sect. **6**·4), or pulses present in counters A or B.

The angles in both views for each track were measured and the space angles calculated. With these angles as particle directions, the four equations resulting from the conservation of four-momentum were solved to obtain the momentum of each particle. The error in the projected angles was $\sim \pm 2^0$, due to multiple Coulomb scattering in the vacuum chamber walls and measurement errors. This error produces an average uncertainty of ± 10 MeV/c in the calculated momentum. The solution was considered as valid if all the momenta were positive and consistent with the observed penetration depth of each particle in a telescope.

Although all the 4-pion events were identified by the above method, events with five or more pions, of which only four were detected by the apparatus, could give a background contribution to reaction (6) by simulating 4-pion events. In order to determine this background contamination, events with five and six pions were generated by means of the Monte Carlo program described in the previous Section. Those that gave an allowed trigger and only four charged particles in the telescopes, were analysed in the same way as $4T$ events. The fractions of events that gave a good fit as a 4-pion event were 12% for $\pi^+\pi^-\pi^+\pi^-\pi^0$ final states and 18% for $\pi^+\pi^-\pi^+\pi^-\pi^{\pm}\pi^{\mp}$ final states. The percentages given above were found to be essentially independent of the total centre-of-mass energy $2E$.

The results of this special analysis are given in Table V. The number of associated WAS events is given (column 2) for each energy at which events were analysed. The number of $4T$ events with no associated γ or pulses in counter A or B is called N_{4T} (column 3). In column 4 are given the numbers of

([30]) F. CERADINI, M. CONVERSI, S. D'ANGELO, K. EKSTRAND, M. GRILLI, E. IAROCCI, M. NIGRO, L. PAOLUZI, R. SANTONICO, P. SPILLANTINI, V. VALENTE and R. VISENTIN: Internal report LNF 72-90 (to be published).

TABLE V. – *Number of 4T events.*

$2E$ (GeV)	WAS	N_{4T}	$N_{4T\,\mathrm{RECONST}}$	$N_{4\pi}$	$N_{(4T+\gamma)}+N_{(4T+A\,\mathrm{or}\,B)}$
1.2	760	0	0	0	0
1.5	2419	12	11	11	1
1.65	992	8	6	6	0
1.9	2164	8	5	5	1
2.1	6187	13	9	6	13
2.4	1101	5	2	1	4

« reconstructed $4T$ events » ($N_{4T\mathrm{reconst}}$); *i.e.* events which were kinematically consistent with the hypothesis of only 4 pions in the final state. The actual numbers of 4π events, $N_{4\pi}$, were obtained by subtracting the background of fake 4π events due to 5π and 6π events from $N_{4T\mathrm{reconst}}$. For the sake of completeness the numbers of $4T$ events with associated γ and/or signals from counters A or B, also are listed in the last column of Table V.

The cross-section for process (6) was calculated from the numbers $N_{4\pi}$ and the results were previously reported ([13]).

These results show an enhancement of the cross-section around $2E = \sim 1.6$ GeV (see Fig. 18), suggesting the possible production of a ρ'-meson ($M_{\rho'} = \sim 1.6$ GeV, $\Gamma_{\rho'} = \sim 350$ MeV). The interpretation of the results reported in this Section will be further discussed in Sect. **10** and **11**.

10. – Analysis and results.

The objective of this Section is to describe the methods used in obtaining partial cross-sections for the reactions (4) through (10). The input data to these calculations are the observed numbers of $2T$, $3T$, $4T$ and $5T$ events, with and without converted photons and pulses in counters A and B. Also utilized are the efficiencies, as determined in Sect. **8**, for each reaction to contribute to these observed configurations.

As mentioned previously (Sect. **5**), most multiparticle events are observed with little if any background. This is particularly true for $3T$, $4T$ and $5T$ events, however for $2T$ events this was true only when the criteria on track penetration were used to suppress gas-beam interactions (see Sect. **5**). A further correction to the number of $2T$ events also was necessary due to several well-known processes, *i.e.*

(11) $\qquad e^+e^- \to \mu^+\mu^-\gamma \quad \text{and} \quad \pi^+\pi^-\gamma\ ,$

(12) $\qquad e^+e^- \to e^+e^-\mu^+\mu^- \quad \text{and} \quad e^+e^-\pi^+\pi^-\ .$

The small number of these events that was detected by our apparatus was estimated [31] to be 16 $2T$ events and accordingly a correction was applied.

The calculation of the partial-reaction cross-sections was made by solving the following system of k equations at each energy $2E$:

$$N_K = \mathscr{L} \sum_A \varepsilon_K^{(A)} \cdot \sigma_A , \tag{13}$$

where

$A = 1, 2, \ldots, 7$ indicates one of the seven reactions (4)-(10) listed in Sect. **7**;

$K = 1, 2, \ldots, 11$ is one of the eleven observed configurations listed in the first row of Table VI ($2T, \ldots, 5T$ configurations);

TABLE VI. – *Summary of the numbers of observed events of each type.*

$2E$ (GeV)	$\mathscr{L}$ (10^{+33} cm^{-2})	Number of events in the following configurations [a]				
		$2T$ (total)	$2T+\gamma$	$2T+A$ or B	$3T$ (total)	$3T+\gamma$
1.2	5.07	9	0	0	3	0
1.5	23.8	33	4	7	38	8
1.65	19.5	—	—	—	17	—
1.9	43.5	42	15	7	35	11
2.1	163.0	83 [b]	14 [b]	22 [b]	122	30
2.4	49.7	—	—	—	23	8

$2E$ (GeV)	$\mathscr{L}$ (10^{+33} cm^{-2})	Number of events in the following configurations [a]					
		$3T+A$ or B	$4T$ (total)	$4T+\gamma$	$4T+A$ or B	$N_{4\pi}$	$5T$
1.2	5.07	0	0	0	0	0	0
1.5	23.8	9	14	1	0	11	1
1.65	19.5	—	8	—	—	6	0
1.9	43.5	12	10	1	0	5	1
2.1	163.0	28	39	2	11	6	6
2.4	49.7	5	13	3	1	1	4

(*a*) Some events are missing because of insufficient background measurements or reduced shower detection efficiency of the spark chambers which occurred during some of the runs.
(*b*) The integrated luminosity corresponding to these categories of events was $\mathscr{L} = 90 \cdot 10^{33}$ cm^{-2}.

[31] G. BARBARINO, F. CERADINI, M. GRILLI, E. IAROCCI, M. NIGRO, L. PAOLUZI, R. SANTONICO, P. SPILLANTINI, L. TRASATTI, V. VALENTE, R. VISENTIN and G. T. ZORN: Frascati-LNF-72/42 (1972).

N_K is the number of events in the configuration K;

σ_A is the cross-section for process A;

$\varepsilon_K^{(A)}$ is the efficiency for detecting process A in the configuration K;

$\mathscr{L}$ is the integrated luminosity.

A standard Monte Carlo method was applied in solving these equations. Taking into account statistical errors for N_K and $\varepsilon_K^{(A)}$, a random search for a χ^2 minimum was made over a range for σ_A from 0 to 100 nb. χ^2 values which did not exceed 1.2 times the number of equations were considered as valid solutions. The average value and variance for each σ_A were determined from the distribution of values satisfying the above χ^2 criterion.

In principle it is possible to solve these equations at each energy and, in general, this was done. However, due to the lack of some information at certain energies, this was not always possible.

The discussion which follows attempts to explain the results as they appear in Table VII, where the quoted statistical errors correspond to one standard deviation.

i) When solving eqs. (13), the measured fractions $(3T+\gamma)/3T$ and $(4T+\gamma)/4T$ are the leading quantities in separately determining the cross-sections $\sigma(2\pi^+2\pi^-\pi^0)$ and $\sigma(2\pi^+2\pi^-2\pi^0)$. The accuracy of such a separation depends on the precision with which the above fractions and the average π^0 detection efficiency of our apparatus are known. Consequently, at energies where for any reason γ's were not detected, it is only possible to give the cross-section for the sum of the two processes, *i.e.* $\sigma_{4c+n} \equiv \sigma(2\pi^+2\pi^-\pi^0) + \sigma(2\pi^+2\pi^-2\pi^0)$. In these cases the systematic error, appearing in parenthesis, was given. It was taken to correspond to the two extreme possibilities of considering only one of the two processes to be present at a time.

ii) The cross-section $\sigma(2\pi^+2\pi^-)$ can be calculated in two substantially different ways:

1) From the number of events with only four pions, $N_{4\pi}$, as deduced in Sect. **9** and given in Table V.

2) By an over-all fit of all data, *i.e.* by solving eqs. (13). This latter method was applied by solving these equations both with and without the equation referring to $N_{4\pi}$.

All the results obtained by these different methods agree, within the errors, showing the internal consistency of our data. The results in Table VII, column 3 (see also Fig. 18) are those derived by this method. At a total energy $2E = 1.2$ GeV, the error values, appearing in parentheses in Table VII, give the limits for $\sigma(\pi^+\pi^-\pi^+\pi^-)$ and σ_{4c+n} when one assumes that all observed $3T$ events

TABLE VII. – *Summary of the cross-sections, given in nanobarns.*

$2E$ (GeV)	σ_{2c+n}	$\sigma(\pi^+\pi^-\pi^+\pi^-)$	$\sigma(\pi^+\pi^-\pi^+\pi^-\pi^0)$	$\sigma(\pi^+\pi^+\pi^+\pi^-\pi^0\pi^0)$
1.2	$(30\pm2)\pm15$	$(\ 3\ \pm\ 3\ )\pm3$		
1.4				
1.5	$(30\pm4)\pm11$	$(18\ \pm\ 3\ )\pm3$	$6\ \pm7$	16 ± 8
1.65		$23\ \pm11$		
1.77				
1.9	$(22\pm5)\pm\ 4$	$5\ \pm\ 2$	$5\ \pm3$	7 ± 3
2.0				
2.1	$(25\pm6)\pm\ 3$	$1.5\pm\ 1.0$	9.5 ± 3.0	3 ± 2
2.4		<4	10^{+7}_{-4}	3 ± 4

$2E$ (GeV)	σ_{4c+n}	$\sigma(\pi^+\pi^-\pi^+\pi^-\pi^+\pi^-)$	$\sigma_{\geqslant 4c}$	σ_{tot}
1.2	$(\ 5\pm5)\pm6$	<1	$(\ 8\pm\ 2)\pm\ 6$	$(38\pm4)\pm16$
1.4			31 ± 15	
1.5	22 ± 7	$3\ \pm3$	$43\pm\ 9$	$(73\pm4)\pm\ 9$
1.65	$(18\pm4)\pm9$	<3	$(41\pm\ 4)\pm10$	
1.77			24 ± 10	
1.9	11 ± 3	3.5 ± 1.5	$19\pm\ 3$	$(44\pm4)\pm\ 4$
2.0			21 ± 11	
2.1	12 ± 3	3.5 ± 1.0	$16\pm\ 3$	$(45\pm9)\pm\ 3$
2.4	13 ± 4	$4\ \pm2$	$16\pm\ 4$	

The definitions used in this Table are as follows:

$$\sigma_{2c+n} = \sigma(\pi^+\pi^-\pi^0) + \sigma(\pi^+\pi^-\pi^0\pi^0)\,,$$

$$\sigma_{\geqslant 4c} = \sigma(e^+e^- \to \text{at least 4 charged } \pi)\,,$$

$$\sigma_{4c+n} = \sigma(\pi^+\pi^-\pi^+\pi^-\pi^0) + \sigma(\pi^+\pi^-\pi^+\pi^-\pi^0\pi^0)\,,$$

$$\sigma_{tot} = \sigma(\pi^+\pi^- + \text{anything})\,.$$

Where two errors are reported, the first, in parenthesis, is the systematic error and the second is the statistical error.

or none were produced by these channels. At $2E = 1.5$ GeV the error in $\sigma(\pi^+\pi^-\pi^+\pi^-)$, appearing in parentheses, depends on the fit procedure; it reflects the fact that the channel $\pi^+\pi^-\pi^+\pi^-\pi^0$, whose cross-section $\sigma(\pi^+\pi^-\pi^+\pi^-\pi^0)$ at this energy is compatible with zero, can be included or not in the calculations.

iii) Many channels produced in the e^+e^- interactions are of the type

$$e^+e^- \to \pi^+\pi^- + n\pi^0 \qquad \text{with } n \geqslant 1,$$

and contribute, therefore, to the same $2T+\gamma$ configuration (*). The information which can be derived from the observed $2T+\gamma$ events is consequently insufficient to separate the various contributions. Nevertheless the observed fraction $(2T+\gamma)/2T$ is small enough to exclude contributions in excess of $\sim 30\,\%$ from channels with $n \geqslant 3$, at any energy. In evaluating the cross-section $\sigma_{2c+n} \equiv \sum_n \sigma(\pi^+\pi^- + n\pi^0)$ these contributions have not been considered, so that

$$\sigma_{2c+n} = \sigma(\pi^+\pi^-\pi^0) + \sigma(\pi^+\pi^-\pi^0\pi^0)\,.$$

The numerical value of σ_{2c+n} reported in column 2 of Table VII is obtained by using as detection efficiency the average value

$$\bar{\varepsilon} = \tfrac{1}{2}[\varepsilon_{2T}^{(\pi^+\pi^-\pi^0)} + \varepsilon_{2T}^{(\pi^+\pi^-\pi^0\pi^0)}]\,.$$

Also in this case, as in the case of σ_{4c+n} considered above, the limits in the quoted systematic error (appearing in parentheses) correspond to assuming that only one of the two reactions is present at a time. Precisely it is found that the lower limit corresponds to considering only the process $e^+e^- \to \pi^+\pi^-\pi^0\pi^0$.

It should be pointed out that experimental information from the « $\gamma\gamma$ group » ([12]), as well as theoretical considerations by various authors (**), suggest that at Adone energies the contribution from the $\pi^+\pi^-\pi^0$ channel to the $(2c+n)$ cross-section is at most a few nanobarn. Assuming that $\sigma_{2c+n} \sim \sigma(\pi^+\pi^-\pi^0\pi^0)$ is, therefore, most probably correct.

The results given in Table VII are also shown in graphical form in Fig. 17-24. Available data from other laboratories ([3b,32]) and/or from other groups working at Adone ([11,12]) also have been reported in the Figures

---

(*) It should be recalled (see Table IV) that the configurations $nT+\gamma$ in a few cases involve the presence of more than one detected γ. For example, the $2T+\gamma$ configuration involves two identified γ in a fraction of cases which is less than 10%. The statistical significance of this additional information is too poor to be exploited in the analysis and consequently was ignored.

(**) Essentially these considerations are based on the hypothesis that the process $e^+e^- \to \pi^+\pi^-\pi^0$ is dominated by the ω or φ tail. (See, for instance, J. LAYSSAC and F. M. RENARD: *Lett. Nuovo Cimento*, **1**, 197 (1971).) This hypothesis appears to be valid up to $2E = 1$ GeV according to the ACO data ([3b]).

([32]) V. E. BALAKIN, G. I. BUDKER, I. B. VASSERMAN, O. S. KOITMAN, L. M. KURDADZE, S. I. MISHNEV, A. P. ONUCHIN, S. I. SEREDNYAKOV, V. A. SIDOROV, A. N. SKRINSKY, G. M. TUMAIKIN, V. F. TURCKIN, A. G. KHABAKPASHEV and J. M. SHATUNOV: *Proceedings of the International Symposium on Electron and Photon Interactions at High Energy* (Ithaca, N. Y., 1971), p. 65. The results reported in Fig. 24 come from a reanalysis of data collected by the quoted group, assuming an equal contribution from the processes $e^+e^- \to \pi^+\pi^-\pi^+\pi^-$ and $\pi^+\pi^-\pi^0\pi^0$. These results have been presented by V. A. SIDOROV: at the *Informal Meeting on Electromagnetic Interactions, Frascati, May 1972.*

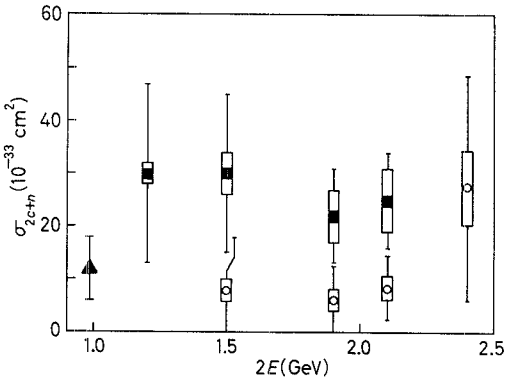

Fig. 17. – Energy dependence of the cross-section $\sigma_{2c+n} = \sigma(\pi^+\pi^-\pi^0) + \sigma(\pi^+\pi^-\pi^0\pi^0)$. The open boxes indicate systematic errors. In our case these errors correspond to assuming only one of the two quoted reactions present at a time. The lower limit corresponds to considering only the process $e^+e^- \to \pi^+\pi^-\pi^0\pi^0$: ■ present experiment, ○ $\gamma\gamma$ group ([12]), ▲ Orsay ([3b]) (only $\pi^+\pi^-\pi^0\pi^0$).

thus improving the information and extending it towards lower energies (*). All these results will be shortly discussed in the next Section. We note here that the systematic errors (given, in our case, in parentheses in Table VII) are indicated by open boxes throughout the Figures. In the case of our data the meaning and the method of estimating systematic errors has

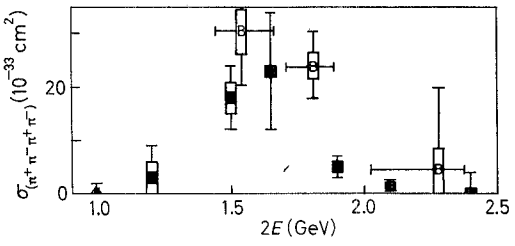

Fig. 18.

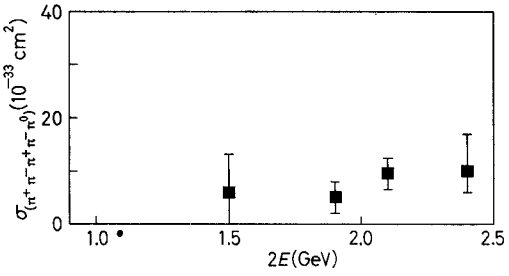

Fig. 19.

Fig. 18. – Energy dependence of the cross-section for the process $e^+e^- \to \pi^+\pi^-\pi^+\pi^-$. Also data from other groups ([3b,11]) are reported for completeness. The points of the present experiment at $2E = 1.2$ and 1.5 GeV include a systematic error indicated by an open box, as in the case of the « boson group » ([11]) results: ■ present experiment, B boson group ([11]), ▲ ACO-Orsay ([3b]).

Fig. 19. – $\sigma(\pi^+\pi^-\pi^+\pi^-\pi^0)$ *vs.* the total energy $2E$.

(*) Values of the cross-section $\sigma_{\geqslant 4c}$ obtained from a re-analysis of data previously reported by BARBIELLINI *et al.* ([33]) are also given in Fig. 23.

been specified above. It should be noticed that these errors do not include the uncertainties in the integrated luminosity $\mathscr{L}$ and in the calculated efficiencies $\varepsilon_K^{(A)}$. A few doubtful events which were disregarded in the course of our analysis

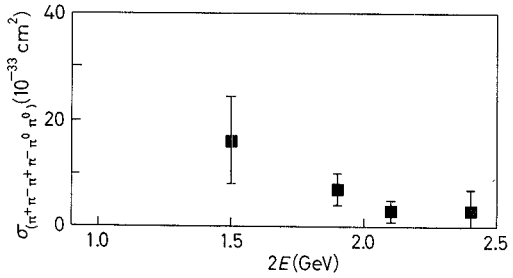

Fig. 20. – $\sigma(\pi^+\pi^-\pi^+\pi^-\pi^0\pi^0)$ *vs.* the total energy $2E$.

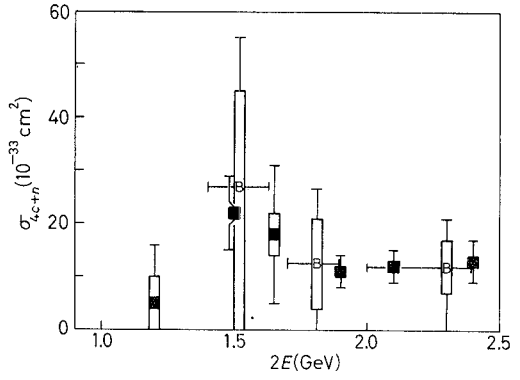

Fig. 21. – Energy dependence of the cross-section $\sigma_{4c+n}=\sigma(\pi^+\pi^-\pi^+\pi^-\pi^0)+\sigma(\pi^+\pi^-\pi^+\pi^-\pi^0\pi^0)$ Also data from the « boson group » ([11]) are shown for comparison. The open boxes indicate systematic errors as in the case of Fig. 17: ▪ present experiment, B boson group ([11]).

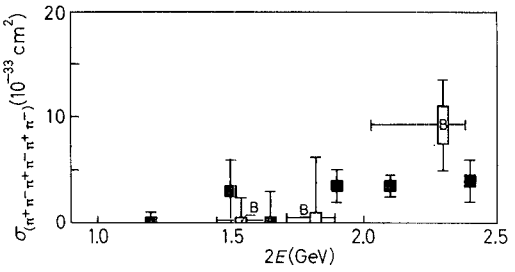

Fig. 22. – $\sigma(\pi^+\pi^-\pi^+\pi^-\pi^+\pi^-)$ *vs.* the total energy $2E$: ▪ present experiment, B boson group ([11]).

(see Sect. 6) could also represent an additional source of error via N_K. We estimate, however, that errors such as those which have been neglected do not exceed in any case the quoted statistical errors, the latter involving, as mentioned already, statistical uncertainties in both $\varepsilon_K^{(A)}$ and N_K.

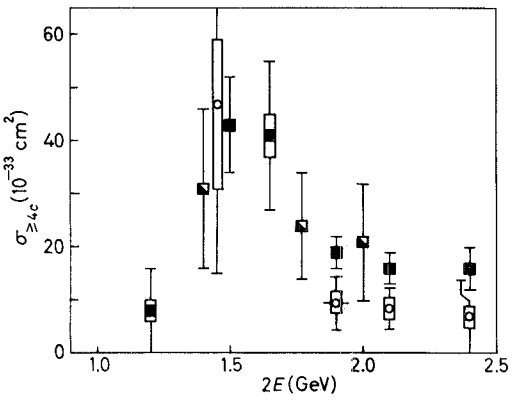

Fig. 23.

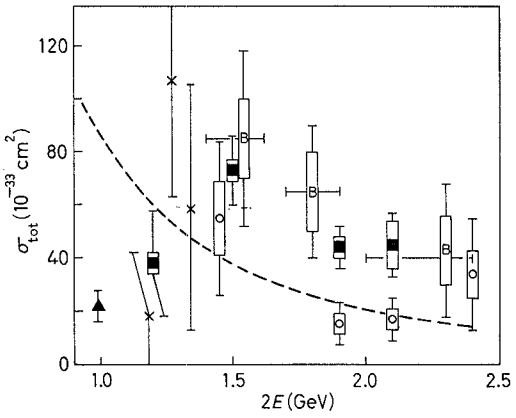

Fig. 24.

Fig. 23. – Energy dependence of the cross-section for processes in which at least four charged pions are produced, with or without neutral pions. It is assumed in our analysis that the maximum multiplicity (charged+neutrals) is six. Data from the «$\gamma\gamma$ group» ([12]) also are reported for comparison. Open boxes indicate systematic errors: ▪ present experiment, ◩ present experiment ref. ([33]), ○ $\gamma\gamma$ group ([12]).

Fig. 24. – Energy dependence of the cross-section for the process $e^+e^- \to \pi^+\pi^- +$ anything. Also data from other groups working with Adone ([11,12]) are shown for comparison. For completeness results from Orsay ([3b]) and Novosibirsk ([32]) are also reported. In each case open boxes indicate systematic errors. The dashed curve, representing the cross-section for $e^+e^- \to \mu^+\mu^-$ (computed from quantum electrodynamics), is shown for reference. ▪ present experiment, B boson group ([11]), ○ $\gamma\gamma$ group ([12]), × Novosibirsk, ▲ Orsay.

It is worth-while noting in the previous Figures that there is substantial agreement between the results obtained by the various groups working at Adone. One noteworthy discrepancy is found for σ_{tot} (Fig. 24) in the region of $2E = 2$ GeV, where the $\gamma\gamma$-group value appears to be somewhat lower than the values measured by the other groups. Slightly lower values are found also, by the same group, for the σ_{2c+n}, as shown in Fig. 17, where the points from the $\gamma\gamma$-group have been computed with $n = 1, 2, 3, 4$. On the other hand, as pointed out already, the lower limit for

([33]) G. BARBIELLINI, M. CONVERSI, M. GRILLI, M. NIGRO, L. PAOLUZI, P. SPILLANTINI, V. VALENTE, R. VISENTIN and G. T. ZORN: *Hadron production by* e^+e^- *colliding beams in the* GeV *region*, presented at the *Informal Meeting on Storage Rings Physics* (Frascati, 1970), unpublished.

σ_{2c+n}, within the systematic errors given in Fig. 17, corresponds to the channel $e^+e^- \to \pi^+\pi^-\pi^0\pi^0$. This is the minimum cross-section we can give, since any mixture of states with a number of π^0's from 1 to 4 would increase the value of σ_{2c+n}: Hence there seems to be a systematic difference between the cross-sections measured by the two groups. We do not believe, however, that great signi-

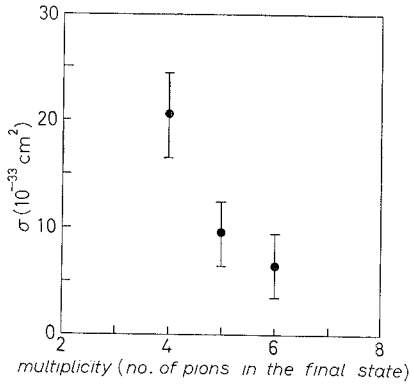

Fig. 25. – The total cross-section for the process $e^+e^- \to \pi^+\pi^-$ + anything as function of multiplicity (*i.e.* total number of charged and neutral pions) at $2E = 2.1$ GeV.

ficance can be attached, at present, to these apparent discrepancies not only because of possible neglected systematic uncertainties, but also because of the differences in the hardware employed in the experiments which produce differences in angular acceptance, energy cut-offs, etc.

In Fig. 25 we report the total cross-section at $2E = 2.1$ GeV as a function

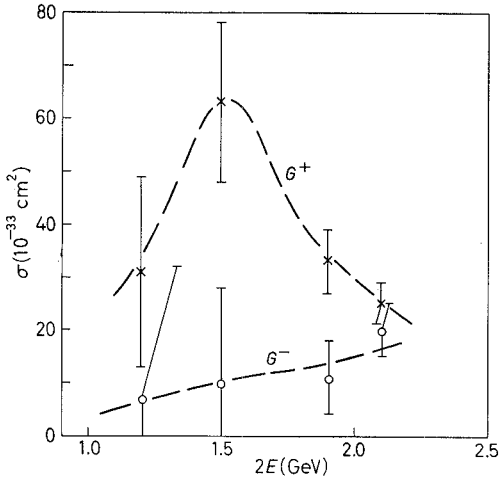

Fig. 26. – Cross-sections for final states with positive and negative G parity *vs.* $2E$: × G^+-parity final states, ○ G^--parity final states.

of the total number of final-state pions (charged plus neutrals). The multiplicity curve has been given explicitly only at this energy, where our results are statistically more significant and, moreover, show no indication of a resonant behaviour. The average multiplicity observed at $2E = 2.1$ GeV is $\langle n_\pi \rangle \sim 4.5$. Furthermore, it does not appear to have any strong energy dependence since $\langle n_\pi \rangle$ has a value between approximately 4 and 5 over the whole energy range explored ($2E = (1.2 \div 2.4)$ GeV).

Finally, in Fig. 26 we report the total cross-section for final states with a positive or a negative G parity. One can see that final states with G^+ parity are much more abundant than those with G^- parity, at least around $2E = 1.5$ GeV.

11. – Discussion and conclusions.

An important conclusion coming from the results reported in the previous Section is that multihadron production, *i.e.* the reaction

$$e^+e^- \to \pi^+\pi^- + \text{anything}, \tag{14}$$

occurs at $2E \geqslant 1.2$ GeV, with a total cross-section σ_{tot} comparable to that for the annihilation process $e^+e^- \to \mu^+\mu^-$, $\sigma_{\mu\mu}$ (Fig. 24). The processes which contribute to reaction (14) seem to have thresholds in the neighbourhood of 1 GeV. Excluding the region below 1.5 GeV, where the cross-section rises rapidly, the energy-dependence of σ_{tot} appears to be consistent, within the large errors, with a $1/E^2$-dependence; even though a less rapid energy-dependence is also compatible with our results in the narrow energy interval explored. In this same energy region ($2E \gtrsim 1.5$ GeV) the ratio $\sigma_{tot}/\sigma_{\mu\mu}$ is apparently greater than 1, possibly close to 2.

The total cross-section σ_{tot} is the sum of many partial cross-sections, which have been evaluated at the various energies explored. The relative weight of these cross-sections depends on the total energy $2E$, as one can see from the Figures of the previous Section. For $2E > 1.5$ GeV the contributions to σ_{tot} (Fig. 24) can be split into two roughly equal parts; one due to processes with only two charged pions plus neutrals (σ_{2c+n}, Fig. 17); the other due to processes with at least four charged pions in the final state ($\sigma_{\geqslant 4}$, Fig. 23). The former contribution, as mentioned already in Sect. **10**, seems essentially to be due to the process:

$$e^+e^- \to \pi^+\pi^-\pi^0\pi^0. \tag{5}$$

On the other hand, the latter contribution comes from the following pro-

cesses:

$$e^+e^- \to \begin{cases} \pi^+\pi^-\pi^+\pi^- , & (6) \\ \pi^+\pi^-\pi^+\pi^-\pi^0 , & (7) \\ \pi^+\pi^-\pi^+\pi^-\pi^0\pi^0 , & (9) \\ \pi^+\pi^-\pi^+\pi^-\pi^+\pi^- , & (10) \end{cases}$$

of which the first three (6), (7) and (9) are responsible for the rise observed in σ_{tot} when $2E$ is greater than ~ 1 GeV.

Of all of the channels that have been studied, the one involving only four charged pions, eq. (6), has the most striking energy-dependence. Its cross-section $\sigma(\pi^+\pi^-\pi^+\pi^-)$ exhibits a broad peak at $2E \simeq 1.6$ GeV (see Fig. 18). This behaviour is suggestive of the production of a vector meson ρ', of mass $m_{\rho'} = \sim 1.6$ GeV/c^2, full width at half-maximum $\Gamma_{\rho'} = \sim 350$ MeV, having the same quantum numbers as the ρ-meson ($J^{PC} = 1^{--}$ and $I^G = 1^+$). Some indication in favour of the possible existence of the ρ'-meson can also be found in the results by DAVIER *et al.* [34] on the photoproduction of four pions by $(6 \div 18)$ GeV γ-rays on protons. Confirming evidence comes from a recent Berkeley-SLAC experiment [35] on four-pion photoproduction in a hydrogen bubble chamber, using linearly polarized monochromatic 9.3 GeV γ-rays obtained by the back scattering of a laser beam [36]. The decay angular distributions as a function of mass, derived from this last experiment, are indeed what would be expected from a ρ' vector meson diffractively produced with helicity conservation.

An attempt can be made to evaluate the coupling constant of the presumed ρ'-meson with the photon ($g_{\rho'\gamma} = em^2_{\rho'}/f_{\rho'}$), by applying the general ideas of the vector-meson-dominance model. Let us assume that the behaviour of $\sigma(\pi^+\pi^-\pi^+\pi^-)$, as plotted in Fig. 18 can be interpreted in terms of a Breit-Wigner curve. The total cross-section at $2E = m_{\rho'}$, σ^{peak}_{all}, for the process $e^+e^- \to \rho' \to$ (all final states) is then related to the coupling constant $f^2_{\rho'}$ by the formula

$$\frac{f^2_{\rho'}}{4\pi} = \frac{4\pi\alpha^2}{m_{\rho'}\Gamma_{\rho'}} \cdot \frac{1}{\sigma^{peak}_{all}} , \qquad (15)$$

where α is the fine-structure constant.

---

[34] M. DAVIER, I. DERADO, D. C. FRIES, F. F. LIU, R. Z. MOZLEY, A. C. ODIAN, J. PARK, W. P. SWANSON, F. VILLA and D. YOUNT: SLAC preprint (June 30, 1971), presented at the *International Symposium on Electron and Photon Interactions at High Energies* (Ithaca, N. Y., 1971).

[35] G. SMADJA, H. H. BINGHAM, W. B. FRETTER, W. J. PODOLSKY, M. S. RABIN, A. H. ROSENFELD, G. P. YOST, J. BALLAM, G. B. CHADWICK, Y. EISENBERG, E. KOGAN, K. C. MOFFEIT, P. SEYBOTH, I. O. SKILLICORN, H. SPITZER and G. WOLF: work presented at the *Experimental Meson Spectroscopy Conference, April, 28-29. Philadelphia, Pa., 1972.*

[36] F. R. ARUTYUNYAN and V. A. TUMANYAN: *Phys. Lett.*, **4**, 177 (1963); R. H. MILBURN: *Phys. Rev. Lett.*, **10**, 75 (1963).

Various assumptions can be made concerning σ_{all}^{peak} in order to estimate $f_{\rho'}^2/4\pi$. We first note the following inequalities:

$$\sigma_{all}^{peak} \geqslant \sigma^{peak}(\pi^+\pi^-\pi^+\pi^-) + \sigma^{peak}(\pi^+\pi^-\pi^0\pi^0) \tag{16}$$

and

$$\sigma^{peak}(\pi^+\pi^-\pi^+\pi^-) + \sigma^{peak}(\pi^+\pi^-\pi^0\pi^0) \geqslant 1.25\sigma^{peak}(\pi^+\pi^-\pi^+\pi^-)\,. \tag{17}$$

The first inequality is obvious, while the second is a consequence of isospin conservation in the reaction $e^+e^- \to$ four pions ([37]).

We can then evaluate $f_{\rho'}^2$ in two different ways:

i) using only the data on the $\pi^+\pi^-\pi^+\pi^-$ channel and both inequalities (16) and (17) we obtain

$$\frac{f_{\rho'}^2}{4\pi} \leqslant 18; \tag{18}$$

ii) taking for $\sigma^{peak}(\pi^+\pi^-\pi^+\pi^-)$ and $\sigma^{peak}(\pi^+\pi^-\pi^0\pi^0)$ the values actually measured (*) at the resonance and using the first inequality we obtain

$$\frac{f_{\rho'}^2}{4\pi} \leqslant 10 \pm 4\,. \tag{19}$$

Assuming $f_{\rho'}^2/4\pi \sim 10$ and taking the value of $f_{\rho}^2/4\pi = 2.54 \pm 0.23$ recently reported by BENAKSAS *et al.* ([3a]), one obtains for the ratio $f_{\rho'}^2/f_{\rho}^2$ a value close to 4. This agrees with the value recently predicted by BRAMON and GRECO ([14]) in their model ([39]) of « extended vector-meson-dominance », EVMD ([40]). These

---

([37]) C. H. LLEWELLYN SMITH and A. PAIS: Report Number COO-3505-21.

(*) In inserting the numerical values for the measured cross-sections in eq. (16) there is an implicit assumption made that the nonresonant background is not greater than the neglected resonant contributions. Such an assumption is in line with what is expected from the model discussed in ref. ([14]) and the ρ tail contribution to the two quoted four-pion channels, as computed in ref. ([38d]).

([38]) See, for example: *a*) G. KRAMER, J. L. URETSKY and F. T. WALSH: *Phys. Rev.*, **3**, 719 (1971); *b*) J. LAYSSAC and F. M. RENARD: *Lett. Nuovo Cimento*, **1**, 197 (1971); *c*) A. M. ALTUKOV and I. B. KHRIPLOVICH: Novosibirsk internal report 36/71; *d*) J. LAYSSAC and F. M. RENARD: Montepellier preprint PM/71/2 (1971); *e*) G. KRAMER: *Electron-positron interactions*, in *Lectures Delivered at 1972 CERN School, Grado, 1972.*

([39]) A. BRAMON and M. GRECO: *Lett. Nuovo Cimento*, **1**, 739 (1971); and Frascati LNF-72/20 (to be published in *Nuovo Cimento*).

([40]) See also: *a*) J. J. SAKURAI and D. SCHILDKNECKT: *Phys. Lett.*, **40** B, 121 (1972); *b*) A. BRAMON, E. ETIM and M. GRECO: Frascati LNF-72/45 (to be published); *c*) T. KOBAYASHI: preprint of Department of Physics, Tokyo University of Education, Tokyo (1972).

authors [14] also predict $(\rho' \to \pi^+\pi^-\pi^+\pi^-)/(\rho' \to \pi^+\pi^-\pi^0\pi^0) \sim 1$. This is in agreement with our results, as can be seen by comparing at $2E = m_{\rho'} \sim 1.6$ GeV $\sigma(\pi^+\pi^-\pi^+\pi^-)$ and $\sigma(\pi^+\pi^-\pi^0\pi^0)$ (which is essentially equal to σ_{2c+n} of Fig. 17, as discussed in Sect. **10**) (*).

It should be pointed out that a direct comparison between these two cross-sections cannot be made except at the ρ' peak, due to possible contributions from $\rho\rho'$ interference. Such an interference might be responsible for the lack of a resonant behaviour in the energy dependence of the measured $\sigma(\pi^+\pi^-\pi^0\pi^0)$ (see Fig. 17).

The hypothesis of a ρ' resonance yields a simple explanation for the relatively large total cross-section of multihadron production in the neighbourhood of 1.6 GeV, since the final states $\pi^+\pi^-\pi^+\pi^-$ and $\pi^+\pi^-\pi^0\pi^0$ represent $\sim 70\,\%$ of σ_{tot}. In this connection it is worth-while pointing out that the hypothesis of a ρ' resonance, with positive G parity (G^+), is also supported by the results displayed in Fig. 26, where, around 1.6 GeV, final states with G^+ parity are seen to be much more abundant than final states with G^- parity (**).

New models of EVMD recently proposed [40] claim the existence of other resonances besides the ρ' (ω' and φ', *e.g.*, as SU_3 partners of the ρ'; and possibly further SU_3 nonets). These higher resonances might be responsible for the large values of σ_{tot} observed at the highest energies attained in our experiment (***). Further measurements are needed, of course, to establish whether these new resonances, including the ρ', do really exist. Should this be the case, the physics of e^+e^- colliding beams in the GeV region would be clearly characterized by these new resonances. On the other hand, if new resonances are not present, there remains the problem of explaining a cross-section which is possibly a factor of 2 larger than the cross-section for $e^+e^- \to \mu^+\mu^-$. A possible explanation can be searched for in terms of the well-known SLAC results on deep inelastic electron-nucleon scattering, where the discovery of a scale-invariant behaviour [42]

(*) In drawing any conclusion on this matter, a word of caution is needed, however, since the $\pi^+\pi^-\pi^0\pi^0$ channel is even less well established experimentally than the channel $\pi^+\pi^-\pi^+\pi^-$. The $\gamma\gamma$ group at Adone, as mentioned earlier, find a somewhat lower value for $\sigma(\pi^+\pi^-\pi^0\pi^0)$ than ours.

(**) The separation into final states of opposite G parity turns out to be useful also for one of the possible comparisons between e^+e^- data at $2E \sim 2$ GeV and data from nucleon-antinucleon annihilation. Recently a specific model has been proposed [41] for such a connection, but unfortunately it predicts a ratio G^+ over G^- states as large as ~ 35; much larger than the one observed (Fig. 26).

([41]) E. PELAQUIER and F. M. RENARD: *Nucl. Phys.*, **39** B, 547 (1972).

(***) Attempts have also been made ([38]) to interpret the multihadron production observed with Adone within the framework of the « classical » vector-meson-dominance model. They do not seem capable, however, of explaining the experimental situation, without introducing very specific and somewhat questionable assumptions.

([42]) E. D. BLOOM, D. H. COWARD, H. DESTAEBLER, J. DREES, G. MILLER, L. W. MO, R. E. TAYLOR, M. BREIDENBACH, J. I. FRIEDMANN, G. H. HARTMANN and H. W. KENDALL:

is very suggestive of a parton structure of the nucleon ([43]). As suggested by various authors ([44]), the connection between colliding beams and deep inelastic results, and therefore significant information on the hadron structure, could be obtained by measuring the following in e^+e^- collisions in the asymptotic region:

i) the energy dependence of the total cross-section for hadron production σ_{tot};

ii) the ratio $\sigma_{tot}/\sigma_{\mu\mu}$;

iii) the energy dependence of hadron multiplicity ([45]).

As an example let us consider point ii), where different theoretical approaches, based on the general concepts of the light-cone and of the quark models have been developed (*). Using the approach based on fundamental *free* spin-$\frac{1}{2}$ quark fields ([46]), one obtains $\sigma_{tot}/\sigma_{\mu\mu} = \frac{2}{3}$. Different values for this ratio are obtained if one introduces elementary-particle constituents, or partons of spin 0 ([47]). The new quark model recently proposed by GELL-MANN ([48]) predicts $\sigma_{tot}/\sigma_{\mu\mu} = 2$, a value which is also predicted by HAN and NAMBU on the basis of a different quark model ([49]). On the other hand, the EVMD model of BRAMON, ETIM and GRECO quoted above ([40]) predicts $\sigma_{tot}/\sigma_{\mu\mu} \sim 1.25$. Unfortunately, at the present stage of this research, the results concerning the

---

Phys. Rev. Lett., **23**, 930 (1969); M. BREIDENBACH, J. I. FRIEDMANN, H. W. KENDALL, E. D. BLOOM, D. H. COWARD, H. DE STAEBLER, J. DREES, J. W. MO and R. E. TAYLOR: *Phys. Rev. Lett.*, **23**, 935 (1969). See also, the rapporteur talk at *Cornell Conference* (1971) by H. W. KENDALL: *Proceedings of the International Symposium on Electron and Photon Interactions at High Energies* (Ithaca, N. Y., 1971), p. 248.

([43]) R. FEYNMAN: *Phys. Rev. Lett.*, **23**, 1415 (1969).

([44]) See, for example, *a*) S. D. DRELL: rapporteur's talk to the *Amsterdam International Conference on Elementary Particles* (Amsterdam, 1971); *b*) R. GATTO: *Evolution of Particle Physics* (New York, London, 1970), p. 138; *c*) B. L. IOFFE and V. A. KHOZE: Yerevan internal report EFI-TF-11 (1970); *d*) R. GATTO and G. PREPARATA: *Nucl. Phys.*, **47** B, 313 (1972).

([45]) On this specific point see, for instance: *a*) J. BJORKEN and S. BRODSKY: *Phys. Rev. D*, **1**, 1416 (1970); *b*) G. ALTARELLI and L. MAIANI: Internal Report ISS 72/8 (Istituto Superiore di Sanità, Roma) (1972); *c*) E. ETIM and Y. SRIVASTAVA: Frascati LNF-72/30 (1972) (submitted for publication to *Phys. Lett.*); *d*) G. PREPARATA: *Proceedings of the Topical Conference on Conformal Invariance* (Frascati, 1972); *e*) R. W. GRIFFITH: Report Bonn University, PT 2-111 (1972). We wish to thank Drs. E. ETIM and Y. SRIVASTAVA for interesting discussions on this subject.

(*) A recent discussion on quark model predictions can be found in H. SUURA, T. F. WALSH and BING-LIN YOUNG: Desy report 72/21 (May 1972).

([46]) See, for example, J. BJORKEN: *Phys. Rev.*, **148**, 1467 (1966); V. GRIBOV, B. L. IOFFE and I. YA. POMERANCHUK: *Phys. Lett.*, **24** B, 554 (1967).

([47]) N. CABIBBO, G. PARISI and M. TESTA: *Lett. Nuovo Cimento*, **4**, 35 (1970).

([48]) M. GELL-MANN: *Schladming Lectures, 1972*,

([49]) M. HAN and Y. NAMBU: *Phys. Rev.*, **139**, 1006 (1965).

absolute value and the energy-dependence of σ_{tot}, as well as the energy dependence of the average multiplicity, cannot discriminate between the different theoretical predictions. This is not only because of the large uncertainties in the measured quantities, but also because there is at present no reason to believe that the asymptotic region has been already reached at Adone energies (*).

In closing the present discussion, we wish to recall that all cross-sections have been calculated assuming invariant phase space only (**). As an indication of the insensitivity of the results to this assumption we have recalculated the cross-section for the process (6) under a quite different hypothesis. Assuming, as an example, that the final state ($\pi^+\pi^-\pi^+\pi^-$) is reached through the intermediate quasi-two-body virtual state $A_1\pi$, ($e^+e^- \to A_1^{\pm}\pi^{\mp} \to \pi^+\pi^+\pi^-\pi^-$), we find a cross-section which, at all energies, does not exceed that obtained assuming invariant phase space by more than 20 %. So we feel that the assumption of invariant phase space adopted throughout our analysis, should not affect the general conclusions reached in the previous discussion.

The principal results of this experiment may be summarized as follows:

1) Multihadron production by e^+e^- beams colliding at GeV energies occurs with a total cross-section σ_{tot} comparable to that of the annihilation process $e^+e^- \to \mu^+\mu^-$, $\sigma_{\mu\mu}$ (see Fig. 24). In particular at the highest energies attained $((2 \div 2.4)\,\text{GeV})$ $\sigma_{tot}/\sigma_{\mu\mu}$ is apparently greater than 1, possibly close to 2.

2) The energy-dependence of σ_{tot} exibhits a fast rise near 1 GeV. For $2E \gtrsim 1.5$ GeV the energy-dependence of σ_{tot} is compatible with $1/s$ ($s = 4E^2$).

3) The average pion multiplicity (charged plus neutral) is found to be between 4 and 5, over the energy range explored. At $2E = 2.1$ GeV, above the ρ' region, the average multiplicity is $\langle n_\pi \rangle \simeq 4.5$ (see Fig. 25).

4) Final states with positive G parity (G^+) are found to be much more abundant than G^- final states (see Fig. 26).

5) G^+ final states are made up mostly of four pions ($\pi^+\pi^-\pi^0\pi^0$ and $\pi^+\pi^-\pi^+\pi^-$), with $\sigma(\pi^+\pi^-\pi^0\pi^0) + \sigma(\pi^+\pi^-\pi^+\pi^-) \simeq 0.7\ \sigma_{tot}$.

6) The energy-dependence of $\sigma(\pi^+\pi^-\pi^+\pi^-)$ is suggestive of a resonance behaviour (see Fig. 18). This may be interpreted in terms of a ρ'-meson of mass $m_{\rho'} \sim 1.6$ GeV/c^2 and $\Gamma_{\rho'} \sim 350$ MeV, coupled to the photon with a coupling constant $g_{\gamma\rho'} = em^2/f_{\rho'}^2$, where $f_{\rho'}^2/4\pi \leqslant 18$.

(*) If this were the case, the observed energy-dependence of the average multiplicity (Sect. **10**) would not be in agreement with the predictions of the particularly simple statistical model proposed by BJORKEN and BRODSKY ([45a]), *i.e.* $\langle n_\pi \rangle \propto E$.

(**) An exception is the cross-section $\sigma(\pi^+\pi^-\pi^0\pi^0)$ measured at ACO ([35]), where the value was derived assuming the specific process $e^+e^- \to \omega^0\pi^0 \to \pi^+\pi^-\pi^0\pi^0$ This value is given in Fig. 17.

7) The existence of the ϱ'-meson would yield a straighforward explanation for the large cross-section around 1.6 GeV. At higher energies other resonances could be invoked, in a resonant model, to explain the relatively large cross-section observed up to the highest total energy attained in this experiment.

* * *

The present experiment was made possible by the active co-operation of the accelerator group at Adone under the leadership of Prof. F. AMMAN. Particular thanks are due to Dr. M. PLACIDI for his continuous efforts in keeping the machine operation as efficient as possible.

We wish to express warmly our gratitude to Prof. G. BARBIELLINI who greatly contributed to the first stage of the experiment. Thanks are also due to Drs. G. BARBARINO and G. GIANNOLI for their partecipation in the analysis of the events; to M. BERTINO, G. NICOLETTI and A. PECCHI for their invaluable help in solving many technical problems, and to E. CECCARELLI and his collaborators for the scanning and analysis of the events.

The important contribution made by the machine shops in Rome and at Frascati, under the guidance of Mr. A. PELLIZZONI and Mr. G. DI STEFANO, respectively, is gratefully acknowledged.

We thank Profs. N. CABIBBO, S. D. DRELL and R. GATTO for illuminating discussions on some of the more fundamental theoretical aspects underlying this research.

Finally, special thanks are due to Drs. A. BRAMON and M. GRECO for their continuous interest and for many valuable conversations which helped to clarify the interpretation of our experimental results.

APPENDIX A

A more complete and detailed description of the apparatus is given in this Appendix [50]. The dimensions of the counters and the kinematic spark chamber C_1, that limit the solid angle, are listed in Table VIII. A complete list of the dimensions of the absorbers and all active elements is given in Table IX (see also Fig. 1).

It should be mentioned that heavy shielding of concrete and lead (~ 40 r.l.) was placed around the telescopes in the horizontal plane, to which the beam losses are mostly confined. To obtain a further reduction of the trigger rate due to machine background, it was also necessary to have 1 radiation length of lead before counters I_1, E_1 and the same amount in front of counters I_2,E_2.

---

[50] For other details we refer the reader to a seminar delivered by one of us (M.C.) at the Erice International School of Subnuclear Physics, in *Elementary Processes at High Energy* (New York, 1971), p. 547.

TABLE VIII. – *Counters and spark chamber limiting the solid angle.*

Element	a (cm)	b (cm)	d (cm)
Counter 0	$\pm$ 30	$\pm$ 13.5	14
Spark chamber C_1	$\pm$ 37	$\pm$ 30	24
Counter 1	$\pm$ 36.5	$\pm$ 30	30
Counter 2	$\pm$ 40	$\pm$ 40	45
Counter 3	$\pm$ 50	$\pm$ 50	64
Counter 4	$\pm$ 60	$\pm$ 60	82

a = horizontal half width,
b = vertical half height,
d = distance from centre of the straight section.

TABLE IX. – *Thickness of elements of the telescope.*

		Material	mm	g/cm² (Fe eq)	Rad. length	Inter. length
Vacuum chamber:	window	Fe	0.2	0.2	0.01	0.001
	body	Fe	6	4.7		
Counter 0		CH	10	1.5	0.02	0.015
Spark chamber C_1		Al	1.8	0.5	0.02	0.006
Absorber		Pb	5	4.3	0.98	0.032
Counter 1		CH	10	1.5	0.02	0.015
Absorber		Pb	5	4.3	0.98	0.032
Čerenkov counter Č		Al	10	3.0	0.11	0.029
		CH	10	1.5	0.02	0.015
		H_2O	60	8.8	0.17	0.074
Counter 2		CH	20	3.0	0.05	0.030
Spark chamber C_2		Fe	19.5	15.2	1.13	0.128
Counter 3		CH	20	3.0	0.05	0.030
Spark chamber C_3		Fe	34	26.5	1.95	0.224
		Al	32	10.0	0.36	0.094
Counter 4		CH	20	3.0	0.05	0.030
Absorber ($\frac{1}{2}$ of $\Delta\Omega$)		Fe	140	110	8.0	0.92
Absorber		Fe	90	70	5.15	0.59
Absorber (shaped)		Fe	140 (max)	110	8.0	0.92
Counter 5		CH	20	3.0	0.05	0.030
Spark chamber C_4 (only one)		Al	15	4.5	0.16	0.043
		Fe	37.5	33.7	2.31	0.29

This last material was actually made up of two water Čerenkov counters $\check{C}_I$, $\check{C}_E$. These counters were not used in the trigger, but their outputs were displayed in the «DATA BOX» and later were used in the analysis (see Sect. **2** and Fig. 27). They were effective in selecting K-meson pairs from π pairs, because the K-meson velocity is below the threshold for producing Čerenkov light for Adone energies up to $2E = 1.5$ GeV.

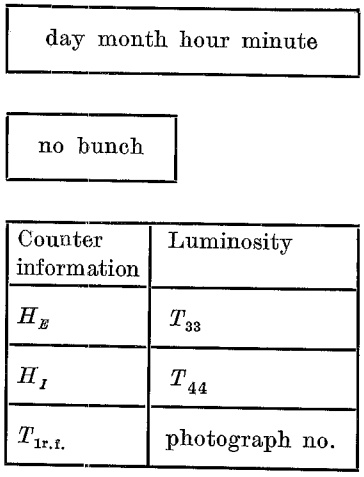

Counter information	octal (coded number)
1st digit:	bit 0: $M_{\mu\mu}$
	bit 1: M_{mh}
	bit 2: D_0
2nd digit:	bit 0: E_3
	bit 1: I_3
	bit 2: E_4
3rd digit:	bit 0: I_4
	bit 1: E_5
	bit 2: I_5
4th digit:	bit 0: $\check{C}_E$
	bit 1: $\check{C}_I$
	bit 2: A
5th digit:	bit 0: B

DATA BOX

Fig. 27. – Information contained in the DATA BOX appeared in the photograph of the two views of the spark chambers.

The presence in the trigger of counters 0 always was required. These counters helped especially in reducing cosmic-ray background for collinear muons ([23]). Each set of counters I_0 and E_0 consisted of three horizontal slabs of scintillators, each one with a photomultiplier tube. Thus, with an appropriate electronic logic described below, in the case of selection of muon pairs, it was possible to narrow down the bounds of the central region surrounding the actual source. All counters, except I_0, E_0, I_1, E_1, had phototubes placed on opposite sides of the scintillator (*e.g.* I_{2R}, I_{2L}, E_{2R}, E_{2L}, etc.) and they were put in coincidences between each other before entering into the rest of the logic. By this arrangement, the efficiency for detecting charged particles in the light pipes was reduced pratically to zero, while the overall efficiency of the scintillator was always $\sim 99\,\%$. This improvement was very helpful, not only to reduce background, but especially to define the active region of the counter itself.

The counters E_3, I_3, E_4, I_4 were employed also to measure the time delay between the opposite pairs, as explained in Sect. 2, and in this case the output pulses from the two sides of the scintillator were used individually in order to minimize the effect of the large dimensions of these counters ([24]).

This time information was processed by fast circuits, in order to be used in the formation of the master trigger. A block diagram is shown in Fig. 28 and a description follows. Pulses from opposite sides of counters I_3, E_3 and I_4, E_4 (*e.g* I_{3L}, E_{3R}, I_{4L}, E_{4L}) were fed to four time-to-amplitude converters (TAC), as START and STOP pulses; the gate pulse was provided in each case by the suitable coincidence (*i.e.* $E_1 \cdot I_1 \cdot E_2 \cdot I_2 \cdot E_3 \cdot I_3$) for the timing between counters 3 and similarly for counters 4.

The outputs of the two time-to-amplitude converters for each opposite pair of counters were linearly mixed and fed to a fast window discriminator. Thus the simultaneous crossing of the counters by collinear particles produced in e^+e^- collisions gave a pulse, the average amplitude of which was midway between the limits imposed by the single-channel discriminator. The same pulse, without any shaping was also converted to digital form and displayed on the DATA BOX for later analysis (see Fig. 11).

Since cosmic rays crossed the counters of each pair with a time delay equal to the distance between them divided by the speed of light (~ 9 ns for counters 3 and ~ 12 ns for counters 4), they will produce two peaks in the time-of-flight spectrum, in the valley between them being located the « good events ». This method, as explained in Sect. **2**, cannot be employed in selecting processes other than μ pair annihilation since it requires particles penetrating until counters 4 in both telescopes. Therefore an alternative trigger employed the veto signal provided by any of the counters E_5, I_5, located in the upper half of the apparatus. The reduction factor in this case was of $\sim 1/40$.

A third method, common to both triggers, was used to reduce the contribution from cosmic rays. A fast coincidence was formed with the phase signal of the accelerating radiofrequency r.f. and the counters E_1 and I_1. The resolution in the prompt coincidence was 20 ns. To improve the discriminating power of this device, we used a time-to-amplitude converter (TAC), the START of which was given by the mixed signals from counters E_1 aud I_1 and the STOP was provided again by r.f. The analog output was digitized and displayed in the DATA BOX. The ultimate resolution (see Fig. 3) was then 4 ns (FWHM), due essentially to the dimensions of counters 1, since the time overlap between the two e^+e^- bunches is about 2 ns.

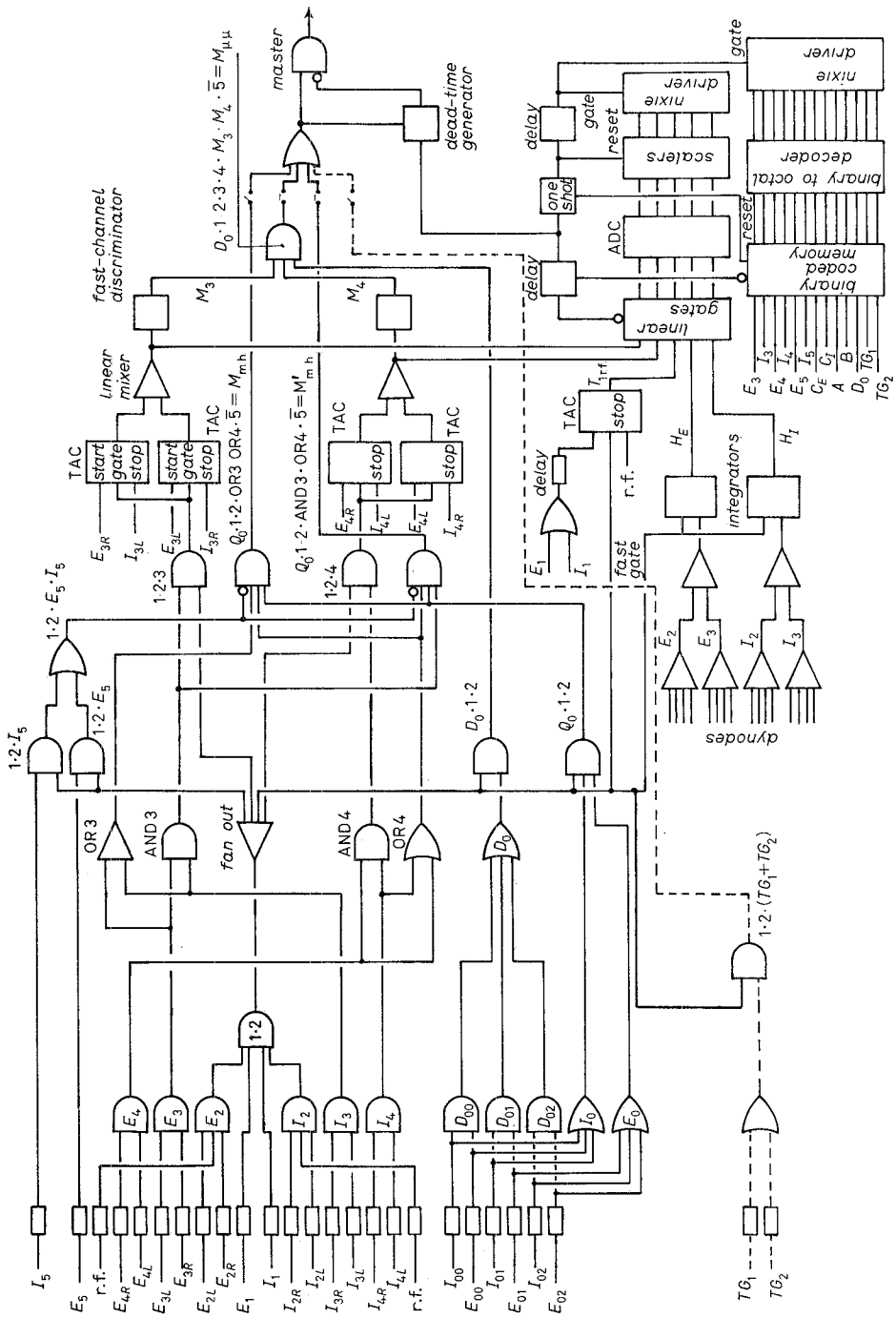

Fig. 28. – Logic-block diagram of fast electronics employed in the experiment.

Finally, the different triggers, formed using alternative logics, were logically mixed in an OR circuit to produce the general master trigger. The two sets of triggers were

$$M_{\mu\mu} = D_0 \cdot 1 \cdot 2 \cdot 3 \cdot 4 \cdot M_3 \cdot M_4 \cdot \text{r.f.}, \tag{A.1}$$

$$M_{\text{m.h.}} = Q_0 \cdot 1 \cdot 2 \cdot (E_3 + I_3) \cdot (E_4 + I_4) \cdot (\overline{E_5 + I_5}) \cdot \text{r.f.}, \tag{A.2}$$

$1, \ldots, 4$ stand for twofold coincidences $E_1 \cdot I_1, \ldots, E_4 \cdot I_4$;

D_0 stands for the « OR » of the three coincidences formed by opposite pairs of 0 counters (*i.e.* $D_0 = (I_{00} \cdot E_{02}) + (I_{01} \cdot E_{01}) + (I_{02} \cdot E_{00})$);

Q_0 stands for the twofold coincidence between any opposite pair of counters 0 (*i.e.* $Q_0 = (E_{00} + E_{01} + E_{02}) \cdot (I_{00} + I_{01} + I_{02})$);

M_3 (M_4) stands for the requirement of no time delay between counters 3 (4).

Because of the machine background at higher energies, the trigger (A.2) was modified in order to maintain the trigger rate of about 1/min. At machine energies greater than $2E = 2$ GeV the trigger (A.2) was then replaced by

$$M'_{\text{m.h.}} = Q_0 \cdot 1 \cdot 2 \cdot 3 \cdot (E_4 + I_4) \cdot (\overline{E_5 + I_5}) \cdot \text{r.f.} \tag{A.3}$$

At machine energies lower than $2E = 1.5$ GeV, it was possible to reduce the energy threshold for a particle to produce a trigger, by excluding counters 4 from the trigger. This fact was especially important for K-mesons, since their range was less than the amount of material before counter 4. The trigger replacing trigger (A.2) was then

$$M''_{\text{m.h.}} = Q_0 \cdot 1 \cdot 2 \cdot (E_3 + I_3) \cdot (\overline{E_5 + I_5}) \cdot \text{r.f.} \tag{A.4}$$

Of course, in the computation of the integrated cross-sections and efficiencies, the different trigger modes were taken into account. Electron pairs were able to produce both kinds of triggers $M_{\mu\mu}$ and $M_{\text{m.h.}}$, thus providing a very convenient means of testing the performance of the apparatus by cross checks on the efficiencies of individual counters.

The master trigger was activating the general gate to open the linear integrators giving the charges collected during 80 ns from $E_2 + E_3(H_E)$ and from $I_2 + I_3(H_I)$. The analog output was displayed in the DATA BOX and a second output was used with a multichannel pulse height analyser to perform occasional tests during data taking and with cosmic rays. The same use also was made of the analog output from T_{33}, T_{44} and $T_{1\text{r.f.}}$, so that the stability of the whole apparatus was under constant control.

A parallel input register (BINARY CODED MEMORY in the block diagram), capable of storing the fast pulses coming from individual counters (see Sect. **2**), was opened on the occurrence of a master trigger. Its binary content was coded in octal form and displayed in the « **DATA BOX** ».

Most of the electronic equipment was installed in the machine hall, at a distance of a few meters from the center of the straight section. During Adone operation, however, no access was permitted into this area, for reasons of radiation safety. Hence, all the checks on the correct operation of the apparatus and related electronics had to be made in the control hall provided for this purpose at a distance of some 20 m. The triggering conditions of the electronics installed in the machine hall could be changed by remote-switching operation, so as to allow one to promptly realize the triggering conditions required for a specific test.

All the relevant information contained in the DATA BOX, was also reproduced in the control hall by means of nixie lamps, which repeated the same numbers appearing in the photograph. A set of scalers giving event number, time interval, and additional useful information also was installed in the control hall. The content of these scalers was automatically printed on paper at regular intervals of 20 min.

The high voltage of the phototube power supplies was automatically reduced to about 1.2 kV whenever the magnetic field of Adone was below a fixed value depending on the machine energy. Therefore during the injection of electrons or positrons into the ring, no damage would result from very intense bursts of particles on the photomultipliers.

On account of the automatic controls mentioned above, continuous presence of physicists or operators was not required during ordinary runs.

The optical system used to bring the two orthogonal views of the apparatus onto the same photographic camera consisted of a set of plane mirrors placed at $\sim 45°$, some of which of very unusual length (~ 4 m). A single frame picture of 70 mm $\times$ 100 mm (Sect. **2**), contained the two stereoviews along with the information given in digital form by the DATA BOX. The demagnification factor was 1/50. The camera, located at 18 m from the centre of the apparatus, was usually loaded with a Ferrania P30 film roll of 120 m, lasting on the average about 10 h.

RIASSUNTO

La produzione multipla adronica da collisioni e^+e^- è stata studiata nell'intervallo di energia totale nel centro di massa da 1.2 a 2.4 GeV. La sezione d'urto totale è confrontabile con quella del processo $e^+e^- \to \mu^+\mu^-$. I processi che contribuiscono alla produzione multipla adronica sembrano innescarsi ad energie totali intorno ad 1 GeV. Sono state ricavate le sezioni d'urto per la produzione di questi diversi processi. L'andamento con l'energia della sezione d'urto del canale $e^+e^- \to \pi^+\pi^-\pi^+\pi^-$ suggerisce l'esistenza di un nuovo mesone vettoriale ρ' ($m_{\rho'} \sim 1.6$ GeV, $\Gamma_{\rho'} \sim 350$ MeV), dotato degli stessi numeri quantici del ρ. È stato stimato un limite superiore per la costante di accoppiamento $f_{\rho'}$ ($f_{\rho'}/4\pi < 18$, ove $f_{\rho'} = m^2_{\rho'} \cdot e/g_{\gamma\rho'}$). Gli stati finali con G parità positiva sono prodotti con maggiore abbondanza di quelli con G parità negativa. La molteplicità media totale (pioni carichi e neutri) è compresa fra 4 e 5 su tutto l'intervallo di energia esplorato.

Многоадронное рождение в e^+e^- соударениях при высоких энергиях.

Резюме (*). — Было исследовано многоадронное рождение на встречных электрон-позитронных пучках для энергий в системе центра масс от 1.2 до 2.4 ГэВ. Полное поперечное сечение, $\sigma_{\text{полн}} = \sigma(e^+e^- \to \pi^+\pi^- + \text{что-либо})$, имеет порядок $\sigma_{\mu\mu} \equiv \sigma(e^+e^- \to \mu^+\mu^-)$, с порогом вблизи 1 ГэВ. Также выводятся парциальные поперечные сечения для различных каналов. Поперечное сечение для канала $e^+e^- \to \pi^+\pi^-\pi^+\pi^-$ обнаруживает энергетическую зависимость, которая дает возможность предположить существование более тяжелого векторного мезона ρ' ($m_{\rho'} \approx 1.6$ ГэВ, $\Gamma_{\rho'} \approx 350$ МэВ), имеющего те же квантовые числа, что и ρ мезон. Приводится верхний предел для константы связи $f_{\rho'}$ ($f_{\rho'}/4\pi < 18$, где $f_{\rho'} = m_{\rho'}^2 e/g_{\gamma\rho'}$). Обнаружено, что конечные состояния с G^+-четностью оказываются много более распространенными, чем конечные состояния с G^--четностью. Получено, что средняя множественность (заряженные плюс нейтральные пионы в конечных состояниях) заключена между 4 и 5 во всей исследованной области энергий.

(*) *Переведено редакцией.*

M. GRILLI, *et al.*
1 Febbraio 1973
Il Nuovo Cimento
Serie 11, Vol. **13** A, pag. 593-644